

Triple excitations in perturbed relativistic coupled-cluster theory and Electric dipole polarizability of group IIB elements

S. Chattopadhyay,¹ B. K. Mani,² and D. Angom³

¹*Department of Physics and Astronomy, Aarhus University, DK-8000 Aarhus C, Denmark*

²*Department of Physics, University of South Florida, Tampa, Florida 33620, USA*

³*Physical Research Laboratory, Ahmedabad - 380009, Gujarat, India*

We use perturbed relativistic coupled-cluster (PRCC) theory to compute the electric dipole polarizabilities α of Zn, Cd and Hg. The computations are done using the Dirac-Coulomb-Breit Hamiltonian with Uehling potential to incorporate vacuum polarization corrections. The triple excitations are included perturbatively in the PRCC theory, and in the unperturbed sector, it is included non-perturbatively. Our results of α , for all the three elements, are in excellent agreement with the experimental data. The other highlight of the results is the orbital energy corrections from Breit interactions. In the literature we could only get the data of Hg [1] and are near perfect match with our results. We also present the linearized equations of the cluster amplitudes, including the triple excitations, with the angular factors.

PACS numbers: 31.15.bw, 31.15.ap, 31.15.A-, 31.15.ve

I. INTRODUCTION

Electric dipole polarizability α of atoms, and ions is an important property to quantify the response to an external electromagnetic field [2]. It is essential to have accurate values of α for atoms, and ions in numerous state of the art experiments to probe fundamental physics, and develop new technologies. An important example is the accurate predictions of black-body radiation shift [3] in optical atomic clocks [4], which has been realized with optical lattice [5], trapped ions [6] and ultracold atoms [7]. In theoretical atomic structure, and properties calculations α serves as an excellent proxy to assess the accuracy of theoretical many-body calculations. In the present work, the studies on the α of Hg serves as an appraisal of the many-body effects important for accurate structure, and properties calculations. This is a prerequisite to study the permanent electric dipole moment of Hg [8] as a signature of parity- and time-reversal violations, and probe physics beyond the standard model of particle physics. Given the importance of α , it has been studied using a variety of many-body methods, and are discussed in a recent review by Mitroy and collaborators [9]. Another reference we have found extremely valuable for our studies on the α of neutral atoms is the Schwerdtfeger's updated Table of α [10], which originally appeared in the chapter by the same author in the collected volume by Maroulis [11]. The table provides an exhaustive list of references on experimental, and theoretical results of α for the electronic ground states of neutral elements.

In the present work we study the α of Zn, Cd and Hg using the perturbed relativistic coupled-cluster (PRCC) theory. It is built upon the coupled-cluster theory (CCT), first developed to address the nuclear many-body problem [12, 13], and later applied to studies on atom and molecules [14]. The CCT, and relativistic version, relativistic coupled-cluster (RCC), are now extensively used in atomic [15–17], molecular [18], nuclear [19], and

condensed matter physics [20] many-body calculations. In the PRCC theory, we add a second set of coupled-cluster amplitudes to account for an additional interaction Hamiltonian. The method is general, and can be adapted with ease to incorporate different forms of interaction Hamiltonians. The detailed descriptions of the theory is provided in a series of our previous works [21–25]. Besides the description of PRCC theory, through these works we had explored the impact of Breit interaction [22], improved diagrammatic evaluations [23], vacuum polarization [24], and triple excitation cluster operators [25] in the unperturbed cluster operators. A related method used for calculating electric dipole polarizabilities is to consider the z -component of the dipole operator and define a set of perturbed cluster operators [26, 27]. In the present work, we report the inclusion of the dominant perturbative triples in the PRCC theory, and improved validation of including Breit interaction in the generation of orbital basis set and PRCC theory. Our earlier works, related to Breit interaction, reported matching the Dirac-Coulomb-Breit SCF energies with previous results. This, however, provides an assessment of the implementation at a coarse grained level. A better comparison would be the orbital energy corrections from the Breit interaction. This is what we demonstrate for Hg, as we could get the data from a previous work [1]. This, we feel, is an important validation of our implementation of Breit interaction.

The important feature of the present work is, it extends, and verify the applicability of PRCC theory in the computation of α to the transition elements. As expected, we get very good results, and we have gained significant insight on the nature of the correlation effects with d sub-shell as the immediate shell below the valence.

The remaining part of the paper consists of five sections. In next section, Section II, we provide a brief discussion on the RCC theory. The description of the linearized RCC and PRCC equations, along with the angular factors, form the principal parts of subsections in this

section. It must be emphasized that the linearized RCC equations include the triple excitation cluster amplitudes, with the representation we introduced in our previous work [25]. The Section III provides a brief description of how to compute α with PRCC, and is followed with an exposition on the computational details in Section IV. The results and discussions are given in Section V. We provide detailed analysis of our theoretical results, and discuss, vis-a-vis previous results, relevant trends and prospects for possible future improvements. We, then, end the main part of the paper with conclusions. In the appendix, we have listed the angular factors of the linearized RCCSDT and PRCC. With these, we feel, interested readers would be able to implement these theories at the linear level without difficulty. For the details on the nonlinear terms, the readers may refer our previous work [22]. The results and equations presented in this work are in atomic units ($\hbar = m_e = e = 1/4\pi\epsilon_0 = 1$). In this system of units the velocity of light is α^{-1} , the inverse of fine structure constant. For which we use the value of $\alpha^{-1} = 137.035\,999\,074$ [28].

II. RELATIVISTIC COUPLED-CLUSTER THEORY

The Dirac-Coulomb-Breit Hamiltonian H^{DCB} provides a good description of neutral atom, and well suited for structure and properties calculations. For an N -electron atom

$$H^{\text{DCB}} = \Lambda_{++} \sum_{i=1}^N [c\alpha_i \cdot \mathbf{p}_i + (\beta_i - 1)c^2 - V_N(r_i)] + \sum_{i < j} \left[\frac{1}{r_{ij}} + g^{\text{B}}(r_{ij}) \right] \Lambda_{++}, \quad (1)$$

where α and β are the Dirac matrices, Λ_{++} is an operator which projects to the positive energy solutions and $V_N(r_i)$ is the nuclear potential. Sandwiching the Hamiltonian with Λ_{++} ensures that the effects of the negative energy continuum states are neglected in the calculations. Another approach, which is better suited for numerical computations, is to use the kinetically balanced finite basis sets [29–32]. We use this method in the present work to generate the orbital basis sets. The last two terms, $1/r_{ij}$ and $g^{\text{B}}(r_{ij})$ are the Coulomb and Breit interactions, respectively. The later, Breit interaction, represents the inter-electron magnetic interactions and is given by

$$g^{\text{B}}(r_{12}) = -\frac{1}{2r_{12}} \left[\alpha_1 \cdot \alpha_2 + \frac{(\alpha_1 \cdot \mathbf{r}_{12})(\alpha_2 \cdot \mathbf{r}_{12})}{r_{12}^2} \right]. \quad (2)$$

The Hamiltonian satisfies the eigen-value equation

$$H^{\text{DCB}}|\Psi_i\rangle = E_i|\Psi_i\rangle, \quad (3)$$

where, $|\Psi_i\rangle$ is the exact atomic state and E_i is the energy of the atomic state. In the presence of external electromagnetic fields, the Hamiltonian is modified with the

addition of interaction terms. For external static electric field, the interaction is $H_{\text{int}} = -\mathbf{d} \cdot \mathbf{E}_{\text{ext}}$, where \mathbf{d} and \mathbf{E}_{ext} are the induced electric dipole moment of the atom and external electric field, respectively. In the remaining part of this section we give a brief description of RCC theory, which we use to compute atomic state $|\Psi\rangle$ and PRCC to account for the effects of H_{int} in the atomic state.

A. Overview of RCC and PRCC theories

In RCC theory we define the ground state atomic wave-function of a closed-shell atom as

$$|\Psi_0\rangle = e^{T^{(0)}}|\Phi_0\rangle, \quad (4)$$

where $|\Phi_0\rangle$ is the reference state wave-function and $T^{(0)}$ is the unperturbed cluster operator. The wave-function is modified when the atom is subjected to an external static electric field \mathbf{E} , and the interaction Hamiltonian is $H_{\text{int}} = -\mathbf{D} \cdot \mathbf{E}$, where \mathbf{D} is the induced electric dipole moment of the atom. In the present work we define the perturbed ground state as

$$|\tilde{\Psi}_0\rangle = e^{T^{(0)} + \lambda \mathbf{T}^{(1)} \cdot \mathbf{E}}|\Phi_0\rangle = e^{T^{(0)}} \left[1 + \lambda \mathbf{T}^{(1)} \cdot \mathbf{E} \right] |\Phi_0\rangle, \quad (5)$$

where $\mathbf{T}^{(1)}$ are the PRCC operators [21, 22]. For an N -electron closed-shell atom $T^{(0)} = \sum_{i=1}^N T_i^{(0)}$ and $\mathbf{T}^{(1)} = \sum_{i=1}^N \mathbf{T}_i^{(1)}$, where i is the order of excitation. In the coupled-cluster single and double (CCSD) excitation approximation [33],

$$T^{(0)} = T_1^{(0)} + T_2^{(0)}, \quad (6a)$$

$$\mathbf{T}^{(1)} = \mathbf{T}_1^{(1)} + \mathbf{T}_2^{(1)}. \quad (6b)$$

The CCSD is a good starting point for structure and properties calculations of closed-shell atoms and ions. In the second quantized representation

$$T_1^{(0)} = \sum_{a,p} t_a^p a_p^\dagger a_a, \quad (7a)$$

$$T_2^{(0)} = \frac{1}{4} \sum_{a,b,p,q} t_{ab}^{pq} a_p^\dagger a_q^\dagger a_b a_a, \quad (7b)$$

$$\mathbf{T}_1^{(1)} = \sum_{a,p} \tau_a^p \mathbf{C}_1(\hat{r}) a_p^\dagger a_a, \quad (7c)$$

$$\mathbf{T}_2^{(1)} = \frac{1}{4} \sum_{a,b,p,q} \sum_{l,k} \tau_{ab}^{pq}(l,k) \{ \mathbf{C}_l(\hat{r}_1) \mathbf{C}_k(\hat{r}_2) \}^1 a_p^\dagger a_q^\dagger a_b a_a, \quad (7d)$$

where t_{\dots} and τ_{\dots} are the cluster amplitudes, a_i^\dagger (a_i) are single particle creation (annihilation) operators and $abc\dots$ ($pqr\dots$) represent core (virtual) single particle states or orbitals. To represent $\mathbf{T}_1^{(1)}$, a rank one operator, we have used the \mathbf{C} -tensor of similar rank $\mathbf{C}_1(\hat{r})$. Coming to $\mathbf{T}_2^{(1)}$, to represent it two \mathbf{C} -tensor operators

of rank l and k are coupled to a rank one tensor operator. In addition, the PRCC clusters are constrained by other selection rules arising from parity and triangular conditions, these are described in our previous work [22].

With the inclusion of $T_3^{(0)}$ the RCC theory incorporates all the correlation effects up to second order in the residual Coulomb interaction. That is, the theory encapsulates all the many-body perturbation theory (MBPT) diagrams [34] which are first and second order in the residual Coulomb interaction. In addition, as it is coupled cluster theory, it incorporates the connected single, double and triple excitations to all order. The leading order contribution to the uncertainty in the calculations arise from the quadruple excitations, which, in MBPT,

first appear at the third order of perturbation.

B. Linearized CCSDT cluster equations

A simplified approximation which incorporates most of the important the many-body effects is the linearized RCCSDT. In this approximation we only consider terms which are zeroth and first order in the cluster operators. The importance of the linearized cluster equations is that, to solve the RCCSDT equations iteratively, we take the solutions as the initial values. The $T_1^{(0)}$, $T_2^{(0)}$ and $T_3^{(0)}$ cluster equations, as described in our previous work, are then

$$\sum_{bq} g_{aq}^{bp} t_b^{pq} + \frac{1}{2} \sum_{bcq} g_{qa}^{bc} (t_{bc}^{qp} - t_{bc}^{pq}) + \sum_{bqr} g_{qr}^{bp} (t_{ba}^{qr} - t_{ab}^{qr}) + \frac{1}{2} \sum_{bcqr} (g_{qr}^{bc} - g_{rq}^{bc}) t_{abc}^{pqr} + (\varepsilon_p - \varepsilon_a) t_a^p = 0, \quad (8)$$

$$\begin{aligned} & \sum_r g_{ar}^{pq} t_b^{r} - \sum_c g_{ab}^{pc} t_c^{q} + \sum_{cd} g_{ab}^{cd} t_{cd}^{pq} + \sum_{rs} g_{rs}^{pq} t_{ab}^{rs} - \sum_{cr} \left[g_{ar}^{cp} t_{cb}^{rq} + g_{rb}^{pc} t_{ac}^{rq} + \frac{1}{2} g_{ar}^{pc} (t_{cb}^{rq} - t_{bc}^{rq}) \right] + \sum_{rcs} (g_{cq}^{rs} - g_{cq}^{sr}) t_{abc}^{prs} \\ & + \frac{1}{2} \sum_{rcd} (g_{cd}^{rb} - g_{dc}^{rb}) t_{acd}^{prq} + \left(\begin{matrix} p \leftrightarrow q \\ a \leftrightarrow c \end{matrix} \right) + (\varepsilon_p + \varepsilon_q - \varepsilon_a - \varepsilon_b) t_{ab}^{pq} + g_{ab}^{pq} = 0, \end{aligned} \quad (9)$$

$$\begin{aligned} & \sum_s g_{sc}^{qr} t_{ab}^{ps} + \sum_d g_{bc}^{dr} t_{ad}^{pq} + \sum_{ds} \left[g_{pd}^{as} (t_{dbc}^{sqr} + t_{bdc}^{sqr}) + g_{pd}^{sb} t_{adc}^{sdr} + g_{dp}^{as} t_{dbc}^{sqr} \right] + \sum_{st} g_{pq}^{st} t_{abc}^{str} + \sum_{de} g_{de}^{ab} t_{dec}^{pqr} + \left(\begin{matrix} p \leftrightarrow q \leftrightarrow r \\ a \leftrightarrow b \leftrightarrow c \end{matrix} \right) \\ & + (\varepsilon_p + \varepsilon_q + \varepsilon_r - \varepsilon_a - \varepsilon_b - \varepsilon_c) t_{abc}^{pqr} = 0. \end{aligned} \quad (10)$$

where, ε_i is the orbital energy of the i th orbital, $i \leftrightarrow j$ represents permutation of the two indexes and $g_{ij}^{kl} = \langle kl | 1/r_{12} + g^B(r_{12}) | ij \rangle$ is the matrix element of the two-electron interaction Hamiltonian. For the cluster amplitudes t_{abc}^{pqr} , we use the representation introduced in our previous work [25]. The representation is symmetric with respect to the interchange of orbital indexes and reduces the number of terms in the equations. So, in the cluster equations, only classes of contractions based on the number of hole (particle) are considered or terms with unique topology of the Goldstone diagrams are considered in the equations. Another equivalent representation of t_{abc}^{pqr} with a different multipole structure is given in the work of Derevianko and collaborators [35].

The Eqs. (15-17) are in terms of the matrix elements of the two-electron interactions. Another representation which is suitable for atomic or ionic systems, and consistent with the expressions in properties calculations is to write the equations in terms of reduced matrix elements. For this consider the matrix element of the electron-electron Coulomb interaction, following the standard multipole decomposition [32, 34, 36]

$$\begin{aligned} \langle pq | \frac{1}{r_{12}} | ab \rangle &= \sum_k \sum_q \begin{pmatrix} j_p & k & j_a \\ -m_p & q & m_a \end{pmatrix} \begin{pmatrix} j_q & k & j_b \\ -m_q & -q & m_b \end{pmatrix} \\ & \times X_C^k(pqab), \end{aligned} \quad (11)$$

where, we have followed the notations in Ref. [32]. In the above expression $X_C^k(pqab)$ is the reduced matrix element or the part of the matrix element which is independent of the magnetic quantum numbers. It is defined as

$$\begin{aligned} X_C^k(pqab) &= \{j_p, j_a, k\} \{j_q, j_b, k\} \Pi^e(\kappa_p \kappa_a k) \Pi^e(\kappa_q \kappa_b k) \\ & (-1)^k \langle j_p || \mathbf{C}^k || j_a \rangle \langle j_q || \mathbf{C}^k || j_b \rangle R_C^k(pqab), \end{aligned} \quad (12)$$

where, $\{j_i, j_j, k\}$ is the triangular condition, $\Pi^e(\kappa_i \kappa_j k)$ is the parity condition that $l_i + l_j + k$ must be even, \mathbf{C}^k is a c-tensor and $R_C^k(pqab)$ is the radial part of the matrix element. The matrix elements of the Breit iteration, $g^B(r_{12})$, may also be written in a similar form. For this let $X_B^k(pqab)$ represents the reduced matrix element of $g^B(r_{12})$ and as a compact notation define

$$g_{ab,k}^{pq} = X_C^k(pqab) + X_B^k(pqab), \quad (13)$$

as the two-electron reduced matrix element corresponding to the multipole k . Based on this definition, the cluster amplitudes must also be defined in terms of the multipole structure, and we use the notation $t_{ab,k}^{pq}$ to represent the component of t_{ab}^{pq} with multipole k . The cluster amplitude equations Eqs. (15-17) are then in terms of reduced matrix elements. To examine the multipole structure of $T_2^{(0)}$, consider the approximation based on the first order in many-body perturbation theory (MBPT).

The cluster amplitude is then

$$t_{ab,k}^{pq} \approx \frac{g_{ab,k}^{pq}}{(\varepsilon_p + \varepsilon_q - \varepsilon_a - \varepsilon_b)}. \quad (14)$$

It must be mentioned here that this is also the expression we use as the initial guess to solve the cluster equations iteratively using a method like Jacobi. In this case, the multipoles k of the cluster amplitudes are identical to the two-electron interactions. The triple cluster amplitudes t_{abc}^{pqr} , however, involves three multipoles and details related to the multipole representation are discussed in

our previous work [25]. A similar description on the cluster equations with the CCSD approximation, in terms of reduced matrix elements, is presented in Ref. [37]. The reference also provides detailed expressions of the angular factors corresponding to each term in the cluster equation. Adopting the notations defined here and representations of t_{abc}^{pqr} discussed in our previous work [25], we use $t_{abc,l_1l_2l_3}^{pqr}$ to represent the cluster amplitudes of $T_3^{(0)}$ in terms of reduced matrix elements. Where, l_i s are the multipoles in the representation of the $T_3^{(0)}$ cluster amplitudes [25]. The cluster equations are then

$$\begin{aligned} & \sum_{bq} \left(A_1 g_{aq,0}^{pb} - A_2 g_{aq,0}^{bp} \right) t_b^q + \sum_{bcqk_1} g_{qa,k_1}^{bc} \left(A_3 t_{bc,k_1}^{qp} - \sum_{k_2} A_4 t_{bc,k_2}^{pq} \right) + \sum_{bqrk_1} g_{qr,k_1}^{bp} \left(A_5 t_{ba,k_1}^{qr} - \sum_{k_2} A_6 t_{ab,k_2}^{qr} \right) \\ & + \frac{1}{2} \sum_{bcqrl_1} \left(A_7 g_{bc,l_1}^{qr} - A_8 g_{bc,l_1}^{rq} \right) t_{abc,0l_1l_1}^{pqr} + (\tilde{\varepsilon}_p - \tilde{\varepsilon}_a) t_a^p = 0, \end{aligned} \quad (15)$$

$$\begin{aligned} & \sum_r B_1 g_{ar,k}^{pq} t_b^r - \sum_c B_2 g_{ab,k}^{pc} t_c^q + \sum_{cdk_1k_2} B_3 g_{ab,k_1}^{cd} t_{cd,k_2}^{pq} + \sum_{rsk_1k_2} B_4 g_{rs,k_1}^{pq} t_{ab,k_2}^{rs} - \sum_{cr} \left(B_5 g_{ar,k_1}^{cp} t_{cb,k}^{rq} + \sum_{k_1k_2} B_6 g_{rb,k_1}^{pc} t_{ac,k_2}^{rq} \right. \\ & + B_7 g_{ar,k}^{pc} t_{cb,k}^{rq} - \sum_{k_1} B_8 g_{ar,k}^{pc} t_{bc,k_1}^{rq} \left. \right) + \sum_{rcsl_1l_2} \left(B_9 g_{rs,l_1}^{cq} - \sum_{k_1} B_{10} g_{sr,k_1}^{cq} \right) t_{acb,kl_1l_2}^{prs} + \frac{1}{2} \sum_{rcdl_1l_2} \left(B_{11} g_{rb,l_1}^{cd} \right. \\ & \left. - \sum_{k_1} B_{12} g_{rb,k_1}^{dc} \right) t_{acd,kl_1l_2}^{prq} + \left(\begin{smallmatrix} p \leftrightarrow q \\ a \leftrightarrow c \end{smallmatrix} \right) + (\tilde{\varepsilon}_p + \tilde{\varepsilon}_q - \tilde{\varepsilon}_a - \tilde{\varepsilon}_b) t_{ab,k}^{pq} + g_{ab,k}^{pq} = 0, \end{aligned} \quad (16)$$

$$\begin{aligned} & \sum_s C_1 g_{sc,l_3}^{qr} t_{ab,l_1}^{ps} + \sum_d C_2 g_{bc,l_3}^{dr} t_{ad,l_1}^{pq} + \sum_{ds} \left[g_{as,l_1}^{pd} \left(C_3 t_{dbc,l_1l_2l_3}^{sqr} + C_4 t_{bdc,m_1m_2l_3}^{sqr} \right) + \sum_{m_1m_2k} C_5 g_{sb,k}^{pd} t_{adc,m_1m_2l_3}^{sdr} \right. \\ & + \sum_k C_6 g_{as,k}^{dp} t_{dbc,l_1l_2l_3}^{sqr} \left. \right] + \sum_{st} \sum_{m_1m_2k} C_7 g_{st,k}^{pq} t_{abc,m_1m_2l_3}^{str} + \sum_{de} \sum_{m_1m_2k} C_8 g_{ab,k}^{de} t_{dec,m_1m_2l_3}^{pqr} + \left(\begin{smallmatrix} p \leftrightarrow q \leftrightarrow r \\ a \leftrightarrow b \leftrightarrow c \end{smallmatrix} \right) \\ & + (\tilde{\varepsilon}_p + \tilde{\varepsilon}_q + \tilde{\varepsilon}_r - \tilde{\varepsilon}_a - \tilde{\varepsilon}_b - \tilde{\varepsilon}_c) t_{abc}^{pqr} = 0, \end{aligned} \quad (17)$$

where A_i , B_i and C_i are the angular factors given in Appendix A-C, and $\tilde{\varepsilon}_i = \epsilon/\sqrt{[j_i]}$ with $[j_i] = 2j_i + 1$. These are the cluster amplitude equations we solve in the LCCSDT theory.

C. Linearized PRCC equations

The details of the Goldstone diagrams and the corresponding algebraic expressions for the PRCC theory with CCSD approximation are discussed in one of our previous works [22]. In a subsequent work [24] we also described the linearized PRCC (LPRCC) equations obtained from the approximation $[\bar{H}_N^{\text{DC}}, \mathbf{T}^{(1)}] \approx [\bar{H}_N^{\text{DC}}, \mathbf{T}^{(1)}]$ and $\bar{H}_{\text{int}} \approx \mathbf{D} + [\mathbf{D}, T^{(0)}]$, where $\bar{H}_{\text{int}} = \exp(-T^{(0)}) H_{\text{int}} \exp(T^{(0)})$. The eigenvalue equation in

the PRCC theory is then

$$[H_N^{\text{DCB}}, \mathbf{T}^{(1)}] |\Phi_0\rangle = \left(\mathbf{D} + [\mathbf{D}, T^{(0)}] \right) |\Phi_0\rangle. \quad (18)$$

The cluster operator equations are as given in ref. [24]. However, in terms of the cluster amplitudes, the equation for the $\mathbf{T}_1^{(1)}$ cluster amplitudes is

$$\begin{aligned} & \mathbf{d}_a^p + \sum_q \mathbf{d}_q^p t_a^q - \sum_b \mathbf{d}_a^b t_b^p + \sum_{bq} \left(\mathbf{d}_q^b \tilde{t}_{ba}^{qp} + \tilde{g}_{qa}^{bp} \tau_b^q \right) \\ & + \sum_{bqr} \tilde{g}_{qr}^{bp} \tau_{ba}^{qr} - \sum_{bcq} g_{qa}^{bc} \tilde{\tau}_{bc}^{qp} + (\varepsilon_p - \varepsilon_a) \tau_a^p = 0, \end{aligned} \quad (19)$$

where $\mathbf{d}_i^j = \langle j | \mathbf{d} | i \rangle$ is the matrix element of the dipole operator, $\tilde{g}_{ij}^{kl} = g_{ij}^{kl} - g_{ji}^{kl} \equiv g_{ij}^{kl} - g_{ij}^{lk}$ is the antisymmetrized matrix element of the two-body interaction and similarly, $\tilde{\tau}$ is the antisymmetrized perturbed cluster amplitudes. The Goldstone diagrams arising from the terms

in the equation are given in Fig. 1. Similarly, the LPRCC equation for the $\mathbf{T}_2^{(1)}$ cluster amplitudes is

$$\begin{aligned} & \left[\sum_r \left(\mathbf{d}_r^{pq} t_{ab}^{rq} + g_{rb}^{pq} \tau_a^r \right) - \sum_c \left(\mathbf{d}_a^{pc} t_{cb}^{pq} + g_{ab}^{pc} \tau_c^p \right) + \sum_{rc} \left(g_{ar}^{pc} \tilde{\tau}_{cb}^{rq} \right. \right. \\ & \left. \left. - g_{rb}^{pc} \tau_{ac}^{rq} - g_{ar}^{cp} \tau_{cb}^{rq} \right) \right] + \left[\begin{matrix} p \leftrightarrow q \\ a \leftrightarrow b \end{matrix} \right] + \sum_{rs} g_{rs}^{pq} \tau_{ab}^{rs} + \sum_{cd} g_{ab}^{cd} \tau_{cd}^{pq} \\ & + (\varepsilon_p + \varepsilon_q - \varepsilon_a - \varepsilon_b) \tau_{ab}^{pq} = 0, \end{aligned} \quad (20)$$

where $\left(\begin{matrix} p \leftrightarrow q \\ a \leftrightarrow b \end{matrix} \right)$ represents terms similar to those in $[\dots]$ but with the combined permutations $p \leftrightarrow q$ and $a \leftrightarrow b$. The Goldstone diagrams arising from the terms in the above equation are shown in Fig. 2. However, as discussed earlier in the case of LCCSDT, it is more appropriate to write the cluster amplitude equations in terms of the reduced matrix elements. For this we define the cluster amplitude of $\mathbf{T}_1^{(1)}$ as $\tau_{a,1}^b$, where the bold face is to in-

dicate that the cluster amplitude correspond to a rank one operator and subscript ‘1’ is to indicate the rank of the operator. As mentioned earlier, the PRCC theory is general and applicable to perturbations with operators of any rank in the electron sector. So, for other forms of perturbations, the index ‘1’ may be replaced with the appropriate rank. This definition effectively subsumes the reduced matrix element of the c -tensor in the definition of $\mathbf{T}_1^{(1)}$ given in Eq. (7c). Similarly, cluster amplitude of $\mathbf{T}_2^{(1)}$ is defined as $\tau_{ab,l_1 l_2}^{pq}$, where l_1 and l_2 are the ranks of the c -tensor operators coupled to a rank one operator. With this definition reduced matrix elements of the c -tensor part of the representation in Eq. (7d) is incorporated to the definition of $\tau_{ab,l_1 l_2}^{pq}$. Following similar procedure as in LCCSDT, the linearized PRCC equations of the cluster amplitudes $\tau_{a,1}^p$ and $\tau_{ab,l_1 l_2}^{pq}$ in terms of reduced matrix elements are

$$\begin{aligned} & \mathbf{d}_{a,1}^p + \sum_q \mathcal{A}_1 \mathbf{d}_{q,1}^p t_a^q - \sum_b \mathcal{A}_2 \mathbf{d}_{a,1}^b t_b^p + \sum_{bq} \mathbf{d}_{q,1}^b \left(\mathcal{A}_3 t_{ba,1}^{qp} - \sum_k \mathcal{A}_4 t_{ab,k}^{qp} \right) + \sum_{bq} \tau_{b,1}^q \left(\mathcal{A}_5 g_{aq,1}^{pb} - \sum_k \mathcal{A}_6 g_{aq,k}^{bp} \right) \\ & + \sum_{bqr} \sum_{m_1 m_2} \tau_{ba,m_1 m_2}^{qr} \left(\mathcal{A}_7 g_{rq,m_2}^{pb} - \sum_k \mathcal{A}_8 g_{qr,k}^{pb} \right) - \sum_{bcq} \sum_{m_1 m_2} \left(\mathcal{A}_9 g_{aq,m_2}^{cb} \tau_{cb,m_1 m_2}^{pq} - \sum_k \mathcal{A}_{10} g_{aq,k}^{cb} \tau_{bc,m_1 m_2}^{pq} \right) \\ & + (\tilde{\varepsilon}_p - \tilde{\varepsilon}_a) \tau_{a,1}^p = 0, \end{aligned} \quad (21)$$

$$\begin{aligned} & \left(\sum_r \mathcal{B}_1 \mathbf{d}_r^{pq} t_{ab,l_2}^{rq} - \sum_c \mathcal{B}_2 \mathbf{d}_a^{pc} t_{cb,l_2}^{pq} + \sum_r \mathcal{B}_3 g_{rb,l_2}^{pq} \tau_a^r - \sum_c \mathcal{B}_4 g_{ab,l_2}^{cq} \tau_c^p + \sum_{rc} \mathcal{B}_5 g_{ar,l_1}^{pc} \tau_{cb,l_1 l_2}^{rq} - \sum_{rc} \sum_{m_1 m_2} \mathcal{B}_6 g_{ar,l_1}^{pc} \tau_{bc,m_1 m_2}^{rq} \right. \\ & \left. - \sum_{rc} \sum_{km_1 m_2} \mathcal{B}_7 g_{rb,k}^{pc} \tau_{ac,m_1 m_2}^{rq} - \sum_{rck} \mathcal{B}_8 g_{ar,k}^{cp} \tau_{cb,l_1 l_2}^{rq} \right) + \left(\begin{matrix} p \leftrightarrow q \\ a \leftrightarrow b \end{matrix} \right) + \sum_{rs} \sum_{km_1 m_2} \mathcal{B}_9 g_{rs,k}^{pq} \tau_{ab,m_1 m_2}^{rs} \\ & + \sum_{cd} \sum_{km_1 m_2} \mathcal{B}_{10} g_{ab,k}^{cd} \tau_{cd,m_1 m_2}^{pq} + (\tilde{\varepsilon}_p + \tilde{\varepsilon}_q - \tilde{\varepsilon}_a - \tilde{\varepsilon}_b) \tau_{ab,l_1 l_2}^{pq} = 0, \end{aligned} \quad (22)$$

where \mathcal{A} and \mathcal{B} are the angular coefficients listed in the Appendix D-E and $\mathbf{d}_{i,1}^j = \langle j || \mathbf{d} || i \rangle$ is the reduced matrix element of the electric dipole operator. In the above equations, unlike in Eqs. (19) and (20), each of the terms are written separately without symmetrization. This is essential as the direct and exchange diagrams have different angular factors and summation indexes.

Although we include $T_3^{(0)}$ in the calculations of the unperturbed cluster equations, in the PRCC theory computations we restrict to single and double approximation. The reasons for this are the large number of cluster amplitudes and a rather involved angular integration for the diagrams associated with $\mathbf{T}_3^{(1)}$. We, however, consider the contributions from approximate $\mathbf{T}_3^{(1)}$ obtained through perturbative calculations. For this we consider the dominant perturbative term, and the details are provided in the next Section.

III. DIPOLE POLARIZABILITY

A. Expression of α in PRCC

The electric dipole polarizability of the ground state of a closed-shell atom is given by

$$\alpha = -2 \sum_I \frac{\langle \Psi_0 | \mathbf{D} | \Psi_I \rangle \langle \Psi_I | \mathbf{D} | \Psi_0 \rangle}{E_0 - E_I}, \quad (23)$$

where $|\Psi_I\rangle$ are the intermediate atomic states and E_I is the energy of the atomic state. Considering that the ground state of a closed-shell atom or ion is even parity, $|\Psi_I\rangle$ must be odd parity states as \mathbf{D} is an odd parity operator. The above expression of α in terms of the PRCC theory is

$$\alpha = - \frac{\langle \Phi_0 | \mathbf{T}^{(1)\dagger} \bar{\mathbf{D}} + \bar{\mathbf{D}} \mathbf{T}^{(1)} | \Phi_0 \rangle}{\langle \Psi_0 | \Psi_0 \rangle}, \quad (24)$$

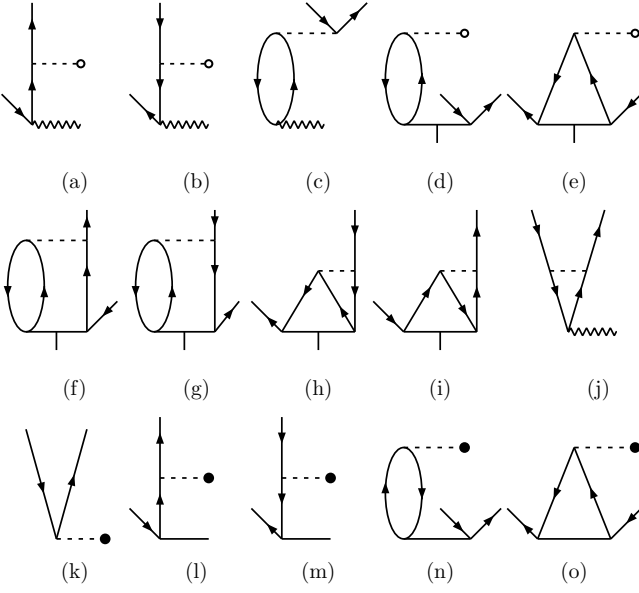


FIG. 1. Goldstone diagrams which contribute to the $\mathbf{T}_1^{(1)}$ equation in the LPRCC approximation. The diagrams (a-c), and (j) arise from $H_N \mathbf{T}_1^{(1)}$, (d-i) arise from $H_N \mathbf{T}_2^{(1)}$, and (k-o) arise from $\mathbf{d} \mathbf{T}^{(1)}$. The dashed lines ending with a circle (o) and filled circle (•) correspond to interactions associated with the single-body part of H_N and H_{int} , respectively. The vertexes with undulating line and a short vertical stump represent $\mathbf{T}_1^{(1)}$ and $\mathbf{T}_2^{(1)}$, respectively.

where, $\bar{\mathbf{D}} = e^{T^{(0)\dagger}} \mathbf{D} e^{T^{(0)}}$, represents the unitary transformed electric dipole operator and $\langle \Psi_0 | \Psi_0 \rangle$ is the normalization factor. Following the derivations presented in our previous works [23, 25], retaining terms up to quadratic in cluster operators, we can write

$$\alpha \approx \frac{1}{\mathcal{N}} \langle \Phi_0 | \mathbf{T}_1^{(1)\dagger} \mathbf{D} + \mathbf{D} \mathbf{T}_1^{(1)} + \mathbf{T}_1^{(1)\dagger} \mathbf{D} \mathbf{T}_1^{(0)} + \mathbf{T}_1^{(0)\dagger} \mathbf{D} \mathbf{T}_1^{(1)} + \mathbf{T}_2^{(1)\dagger} \mathbf{D} \mathbf{T}_1^{(0)} + \mathbf{T}_1^{(0)\dagger} \mathbf{D} \mathbf{T}_2^{(1)} + \mathbf{T}_1^{(1)\dagger} \mathbf{D} \mathbf{T}_2^{(0)} + \mathbf{T}_2^{(0)\dagger} \mathbf{D} \mathbf{T}_1^{(1)} + \mathbf{T}_2^{(1)\dagger} \mathbf{D} \mathbf{T}_2^{(0)} + \mathbf{T}_2^{(0)\dagger} \mathbf{D} \mathbf{T}_2^{(1)} | \Phi_0 \rangle, \quad (25)$$

where $\mathcal{N} = \langle \Phi_0 | \exp[T^{(0)\dagger}] \exp[T^{(0)}] | \Phi_0 \rangle$ is the normalization factor, which involves a non-terminating series of contractions between $T^{(0)\dagger}$ and $T^{(0)}$. In the present work we use $\mathcal{N} \approx \langle \Phi_0 | \mathbf{T}_1^{(0)\dagger} \mathbf{T}_1^{(0)} + \mathbf{T}_2^{(0)\dagger} \mathbf{T}_2^{(0)} | \Phi_0 \rangle$. It must be mentioned here that, as discussed in our previous work [25], the expression of α involves only connected diagrams and the normalization factor is essential. From the above expression of α , an evident advantage of calculation using PRCC theory is the absence of summation over $|\Psi_I\rangle$. The summation is subsumed in the evaluation of the $\mathbf{T}^{(1)}$ in a natural way. This is one of the key advantage of using PRCC theory.

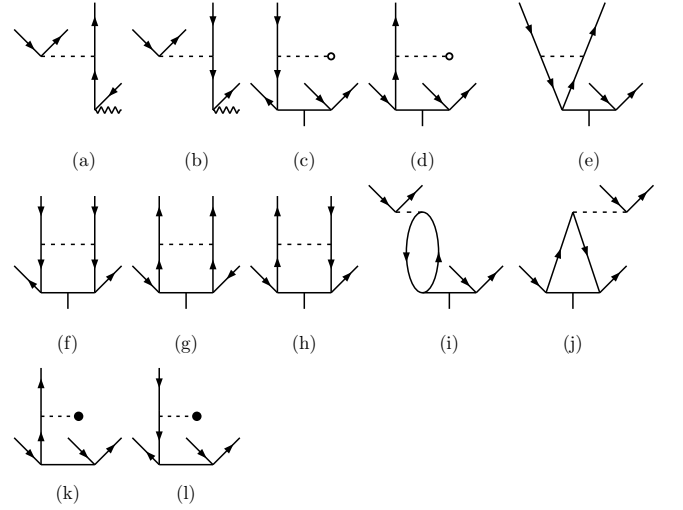


FIG. 2. Goldstone diagrams which contribute to the $\mathbf{T}_2^{(1)}$ in the LPRCC approximation. The diagrams (a-b), (c-j), and (k-l) arise from $H_N \mathbf{T}_1^{(1)}$, $H_N \mathbf{T}_2^{(1)}$, and $\mathbf{d} \mathbf{T}_2^{(1)}$, respectively. The dashed lines ending with a circle (o) and filled circle (•) correspond to interactions associated with the single-body part of H_N and H_{int} , respectively. The vertexes with undulating line and a short vertical stump represent $\mathbf{T}_1^{(1)}$ and $\mathbf{T}_2^{(1)}$, respectively.

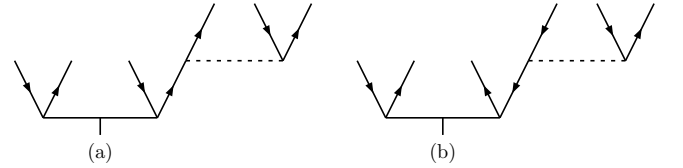


FIG. 3. Goldstone diagrams of approximate $\mathbf{T}_3^{(1)}$ obtained from perturbing $\mathbf{T}_2^{(1)}$ with one order of the electron-electron interaction $g = 1/r_{12} + g_{12}^B$, represented by dashed lines in the diagrams.

B. Perturbative $\mathbf{T}_3^{(1)}$ and α

To obtain the dominant contributions from the triple excitation cluster operators in PRCC, $\mathbf{T}_3^{(1)}$, we consider the perturbative approximation. In this scheme $\mathbf{T}_3^{(1)}$ is approximated as a first order perturbation to $\mathbf{T}_2^{(1)}$, and it accommodates the leading order terms in the cluster amplitude equations of $\mathbf{T}_3^{(1)}$. There are two diagrams in this approximation and are shown in Fig. 3, and these combine to give the perturbative triple excitation cluster amplitude

$$\tau_{abc}^{pqr} \approx \frac{1}{\Delta \epsilon_{pqr}^{abc}} \left(\sum_s \tau_{ab}^{ps} g_{sc}^{qr} - \sum_d \tau_{ad}^{pq} g_{bc}^{dr} \right), \quad (26)$$

where, $\Delta \epsilon_{pqr}^{abc} = \epsilon_p + \epsilon_q + \epsilon_r - \epsilon_a - \epsilon_b - \epsilon_c$, and as defined earlier $g_{ij}^{kl} = \langle kl | 1/r_{12} + g_{12}^B | ij \rangle$. The first and second term on the right hand side of the above equation correspond to the Goldstone diagrams in Fig. 3(a) and (b), respectively.

tively. Each of these diagrams, after contraction with $T_2^{(0)\dagger}$ and \mathbf{D} , generate sixteen diagrams of α each. For example, the set of the sixteen diagrams arising from the perturbative $\mathbf{T}_3^{(1)}$ represented by Fig. 3(a) are shown in Fig. 4. The other term associated with $\mathbf{T}_3^{(1)}$ which contributes to α is $T_1^{(0)\dagger}T_1^{(0)\dagger}\mathbf{D}\mathbf{T}_3^{(1)}$. We, however, neglect this as it is second order in $T_1^{(0)\dagger}$ and expect the contribution to be smaller than $T_1^{(0)\dagger}\mathbf{D}\mathbf{T}_2^{(1)}$, which as we shall discuss later has the smallest contribution in the expression of α in Eq. (25). Here after, the values of α obtained with the inclusion of perturbative $\mathbf{T}_3^{(1)}$ are referred to as PRCC(T).

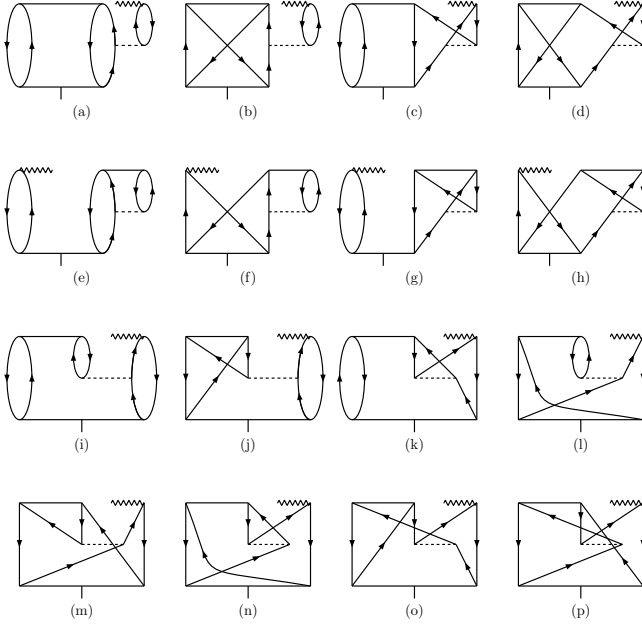


FIG. 4. Diagrams of α which arise from, $T_2^{(0)\dagger}\mathbf{D}\mathbf{T}_3^{(1)}$, which represents the perturbative $\mathbf{T}_3^{(1)}$ contracted with $T_2^{(0)\dagger}$ and \mathbf{D} . The $\mathbf{T}_3^{(1)}$, considered in the diagrams, is obtained from particle-particle contraction of $\mathbf{T}_2^{(1)}$ and electron-electron interaction Hamiltonian $g = 1/r_{12} + g_{12}^B$, represented by dashed lines in the diagrams.

IV. COMPUTATIONAL DETAILS

A. Basis set and nuclear density

We use Gaussian type orbitals (GTOs) [38], and the details relevant to the use of GTOs in RCC and PRCC are described in our previous works [21, 23]. The GTOs are finite basis set orbitals and are the linear combinations of Gaussian type functions (GTFs). The exponents of the GTFs are defined in terms of two parameters α_0 and β . We consider even tempered basis set, or in other words, different α_0 and β for orbitals of each j . We also use kinetic balance condition [29] to obtain small compo-

nents of the orbitals from the large component. Further more, it is appropriate to incorporate Breit interaction [39] in the generation of GTOs as the present study includes Hg, a high Z atom. For this the works of Quiney [40] and Mohanty [38], and their collaborators are excellent references. Keeping in view the implementations general and incorporating mathematically intricate interaction Hamiltonians, for example, the Uehling potential, we generate the GTOs on a grid [41] with V^N potential. The basis parameters α_0 and β are optimized by matching the orbital and self-consistent field (SCF) energies obtained from GRASP2K [42] with the Dirac-Coulomb Hamiltonian. The values of the optimized parameters of Zn, Cd and Hg are listed in Table. I.

TABLE I. The α_0 and β parameters for the s , p and d orbitals of the even tempered GTO basis used in the present calculations.

Atom	s		p		d	
	α_0	β	α_0	β	α_0	β
Zn	0.0385	2.045	0.1095	2.035	0.0091	2.010
Cd	0.0505	2.101	0.0775	1.985	0.0340	1.950
Hg	0.0505	2.045	0.1019	2.223	0.0380	2.050

The SCF energies E_{SCF} obtained with the optimized basis parameters are listed in Table. II. It is evident from the table that E_{SCF} from the GTOs are in very good agreement with the results of GRASP2K, which solves the Dirac-Hartree-Fock equations numerically. An important step in generating the orbitals with GRASP2K is, we use the Hartree-Fock orbitals [43] as the starting values of GRASP2K to improve convergence. As mentioned earlier, we also compare the orbital energies for basis parameter optimization. The details of these comparisons are presented and described in the results and discussions section.

TABLE II. The Dirac-Coulomb SCF energies E_{SCF} of Zn, Cd and Hg obtained from GRASP2K [42] and using Gaussian type orbitals are listed. The Breit interaction corrections to SCF energy $\Delta E_{\text{Br}}^{\text{SCF}}$ are computed using the Gaussian type orbitals. All the values are in atomic units (hartree).

Atom	E_{SCF}		$\Delta E_{\text{Br}}^{\text{SCF}}$	
	GTO	GRASP2K	Present	Ref. [44]
Zn	-1794.6127	-1794.6127	-0.7610	-0.7610
Cd	-5593.3188	-5593.3184	-3.8389	-3.8389
Hg	-19648.8243	-19648.8580	-22.6328	-22.6325

To generate the nuclear potential $V_N(r)$, we use two-parameter finite size Fermi density distribution of the nucleus

$$\rho_{\text{nuc}}(r) = \frac{\rho_0}{1 + e^{(r-c)/a}}, \quad (27)$$

where, $a = t4 \ln(3)$. The parameter c is the half charge radius so that $\rho_{\text{nuc}}(c) = \rho_0/2$ and t is the skin thick-

ness. Using the orbital basis set, we can then solve the RCC and PRCC equations with standard linear algebra method. For efficient parallel implementation we solve the equations iteratively using Jacobi method. It is, however, a method with slow convergence, so employ direct inversion in the iterated subspace (DIIS) [45] to improve convergence.

B. Breit and vacuum polarization corrections

In the present work, we use the general expressions of Breit interaction integrals listed in the work of Grant [46]. To examine the corrections to orbital energies arising from the Breit interactions, we generate the orbitals as solutions of two slightly different single particle equations. In the first case, the orbitals $|\psi_i\rangle$ are computed with the Dirac-Hartree-Fock (DHF) potential and solutions of the equation,

$$(h_0 + U_{\text{DHF}}) |\psi_i\rangle = \epsilon_i |\psi_i\rangle,$$

where, $h_0 = c\boldsymbol{\alpha} \cdot \mathbf{p} + (\beta - 1)c^2 - V_N(\mathbf{r})$ is the single particle part of Dirac-Coulomb Hamiltonian, $|\psi_i\rangle$ is a four component orbital and ϵ_i is the corresponding eigenvalue. The DHF potential in the above equation is defined as

$$U_{\text{DHF}} |\psi_i\rangle = \sum_c^{\text{core}} \left[\langle \psi_c | \frac{1}{r_{12}} (1 - P_{12}) |\psi_c\rangle |\psi_i\rangle \right], \quad (28)$$

where, P_{12} is the permutation operator to represent the exchange integral, c represents core orbitals and ‘core’ indicates sum over all the core orbitals. This implies that the core orbitals are solutions of a set of coupled integro-differential equations and solved using self-consistent-field (SCF) methods. In the second case, we compute the orbitals $|\psi'_i\rangle$ with the Dirac-Hartree-Fock-Breit (DHF_B) potential. The orbitals are then the solutions of the single particle equation

$$(h_0 + U_{\text{DHF_B$$

where, ϵ'_i is the eigenvalue with the DHFB potential, and $U_{\text{DHF_{B is obtained by adding g_{12}^{B} to the central potential in Eq. (28). From the solutions we define the correction to orbital energies due to Breit interaction as}$

$$\Delta\epsilon_{\text{Br}(i)} = \epsilon'_i - \epsilon_i. \quad (29)$$

In a similar way, we also compute the correction due to Uehling potential $\Delta\epsilon_{\text{Ueh}}$.

From the two sets of the orbitals, we define two many-particle ground state reference $|\Phi_0\rangle$ and $|\Phi'_0\rangle$, which are determinantal states consisting of $|\psi_c\rangle$ and $|\psi'_c\rangle$ orbitals, respectively. Based on these states, the SCF energy correction due to Breit interaction is

$$\Delta E_{\text{Br}}^{\text{SCF}} = \langle \Phi'_0 | H^{\text{DCB}} | \Phi'_0 \rangle - \langle \Phi_0 | H^{\text{DC}} | \Phi_0 \rangle, \quad (30)$$

where, H^{DC} is the Dirac-Coulomb Hamiltonian: the Hamiltonian H^{DCB} defined in Eq. (1) without the Breit

interaction. The values of $\Delta E_{\text{Br}}^{\text{SCF}}$ for Zn, Cd and Hg are listed in Table. II, and are near perfect match with the values reported in a previous work [44]. This is another important comparison which validates the choice of the optimized basis set parameters used in the present study. In the results and discussions section, we present $\Delta\epsilon_{\text{Br}}$ of Zn, Cd and Hg orbitals. For the first two atoms, Zn and Cd, we were unable to get previous results from the literature. However, for Hg a previous work [1] has provided the values of $\Delta\epsilon_{\text{Br}}$, and our results are in excellent agreement with those values.

Another way to quantify the effect of Breit interaction is to calculate the first order correction to the SCF energy as

$$\langle H^{\text{B}} \rangle_{\text{DF}} = \langle \Phi_0 | \sum_{i < j} g^{\text{B}}(r_{ij}) | \Phi_0 \rangle. \quad (31)$$

In a previous work [22], we have reported $\langle H^{\text{B}} \rangle_{\text{DF}}$ for the noble gas atoms, and computations were based on the compact expressions of Breit interaction integrals listed in the work of Grant and McKenzie [47]. The computation of $\langle H^{\text{B}} \rangle_{\text{DF}}$ is well suited for testing the implementation of Breit interactions. In the present work, as we have incorporated Breit interaction in the GTO generation and coupled-cluster codes, we give our results of $\Delta E_{\text{Br}}^{\text{SCF}}$ and $\Delta\epsilon_{\text{Br}}$, but not the values of $\langle H^{\text{B}} \rangle_{\text{DF}}$. It must be mentioned here that, among the previous works on Breit interactions, there is another approach to evaluate the Breit interaction matrix elements reported in the work of Mann and Johnson [48]. It is based on the coupling of the Dirac matrices with the angular part of the orbitals. In contrast, the expressions of Grant and collaborators, which we have used, are based on the expansion of $g^{\text{B}}(r_{12})$ as linear combination of irreducible tensor operators.

V. RESULTS AND DISCUSSIONS

The elements of the group IIB studied in the present work, have filled ns orbitals as valence shells and in this regard, similar to the neutral alkaline-earth-metal atoms. There is, however, an important difference: in the group IIB elements the filled $(n-1)d$ shells are the highest energy core orbitals and we can expect significant contribution to the correlation effects from the electrons in the $(n-1)d$ shell. This is indeed the case and is reflected in the identification of the occupied orbitals with dominant contributions to the leading order (LO) term, $\mathbf{T}_1^{(1)\dagger} \mathbf{D} + \text{H.c.}$, in α . We also examine the trends in the contribution from Breit-interaction to the energies of the occupied orbitals. For better description the results for each of the elements (Zn, Cd and Hg) are discussed separately. All the values of α are in atomic units, that is in units of a_0^3 , where a_0 is the Bohr radius.

TABLE III. Orbital energies of Zn and Cd obtained from GRASP2K [42] and Gaussian type orbitals in atomic units (hartree). Here [x] represents multiplication by 10^x .

Orbital	GRASP2K	DC	$\Delta\epsilon_{Br}$	$\Delta\epsilon_{Ueh}$
Zn				
$1s_{1/2}$	-357.7486	-357.7486	4.364[-1]	-2.174[-2]
$2s_{1/2}$	-45.3461	-45.3461	3.129[-2]	-2.125[-3]
$2p_{1/2}$	-39.7403	-39.7402	5.524[-2]	1.724[-4]
$2p_{3/2}$	-38.8513	-38.8513	3.586[-2]	1.859[-4]
$3s_{1/2}$	-5.8000	-5.7999	3.301[-3]	-3.113[-4]
$3p_{1/2}$	-3.9579	-3.9578	5.896[-3]	3.201[-5]
$3p_{3/2}$	-3.8372	-3.8371	3.135[-3]	3.419[-5]
$3d_{3/2}$	-0.7709	-0.7709	2.015[-4]	2.470[-5]
$3d_{5/2}$	-0.7547	-0.7547	-8.255[-4]	2.453[-5]
$4s_{1/2}$	-0.2986	-0.2986	1.251[-4]	-1.080[-5]
Cd				
$1s_{1/2}$	-987.3591	-987.3580	2.017	-1.519[-1]
$2s_{1/2}$	-149.8044	-149.8032	1.810[-1]	-1.702[-2]
$2p_{1/2}$	-139.0231	-139.0218	3.117[-1]	5.952[-4]
$2p_{3/2}$	-131.9158	-131.9145	2.109[-1]	1.006[-3]
$3s_{1/2}$	-29.3222	-29.3212	2.465[-2]	-3.239[-3]
$3p_{1/2}$	-24.9552	-24.9541	4.581[-2]	1.674[-4]
$3p_{3/2}$	-23.6459	-23.6451	2.743[-2]	2.552[-4]
$3d_{3/2}$	-16.0009	-16.0001	1.231[-2]	2.389[-4]
$3d_{5/2}$	-15.7383	-15.7374	4.173[-3]	2.344[-4]
$4s_{1/2}$	-4.7469	-4.7460	3.487[-3]	-5.810[-4]
$4p_{1/2}$	-3.2707	-3.2698	6.390[-3]	5.666[-5]
$4p_{3/2}$	-3.0461	-3.0451	3.141[-3]	7.209[-5]
$4d_{3/2}$	-0.7383	-0.7374	8.961[-5]	5.591[-5]
$4d_{5/2}$	-0.7089	-0.7080	-8.777[-4]	5.506[-5]
$5s_{1/2}$	-0.2814	-0.2810	1.930[-4]	-3.273[-5]

A. Zn

The corrections to the orbitals energies $\Delta\epsilon_{Br}$ and $\Delta\epsilon_{Ue}$ arising from Breit-interaction and Uehling potential, respectively, are listed in Table. III. From the table it is evident that the Breit-interaction tends to *relax* the orbitals as $\Delta\epsilon_{Br}$ is positive in all the cases except $3d_{5/2}$. For the latter, $\Delta\epsilon_{Br(3d_{5/2})}$, is negative and indicates contraction of the orbital. In absolute terms the value of -8.255×10^{-4} hartree for $\Delta\epsilon_{Br(3d_{5/2})}$ is small but the magnitude is larger than $\Delta\epsilon_{Br(3d_{3/2})}$. As to be expected, the deeper core orbitals or orbitals with lower principal quantum number n have larger $\Delta\epsilon_{Br}$ and there is a three orders of magnitude difference between the values of $\Delta\epsilon_{Br}$ for $1s$ and $4s$.

The energy correction arising from the Uehling potential $\Delta\epsilon_{Ue}$ are also listed in Table. III. It is evident that Uehling potential tends to contract the s orbitals as $\Delta\epsilon_{Ue}$ of these orbitals are negative. On the other hand, the occupied orbitals of other symmetries (p and d) *relax* and are indicated by the positive values of $\Delta\epsilon_{Ue}$. This trend is similar to the results of doubly ionized alkaline-earth-metals Mg^{2+} , Ca^{2+} , Sr^{2+} , and Ba^{2+} reported in our previous work [24]. In terms of magnitude, the values of $\Delta\epsilon_{Ue}$ are on average an order of magnitude smaller than $\Delta\epsilon_{Br}$.

From Table. III, it is evident that the basis set pa-

TABLE IV. Convergence pattern of α for Zn and Cd as function of the basis set size. The values of α are in atomic units (a_0^3).

No. of orbitals	Basis size	α
Zn		
113	(15s, 13p, 11d, 9f, 9g, 7h)	38.722
135	(17s, 15p, 15d, 10f, 10g, 9h)	38.717
153	(19s, 17p, 17d, 11f, 11g, 11h)	38.716
171	(21s, 19p, 19d, 13f, 13g, 11h)	38.716
Cd		
99	(15s, 12p, 11d, 7f, 6g, 6h)	49.421
121	(17s, 14p, 13d, 9f, 8g, 8h)	49.135
143	(19s, 16p, 15d, 11f, 10g, 10h)	49.113
165	(21s, 18p, 17d, 13f, 12g, 12h)	49.112
Hg		
112	(12s, 11p, 11d, 11f, 9g, 8h)	33.513
134	(14s, 13p, 13d, 13f, 11g, 10h)	33.499
167	(17s, 16p, 16d, 16f, 14g, 13h)	33.499
178	(18s, 17p, 17d, 17f, 15g, 14h)	33.499

rameters reproduces the numerical values of the orbital energies, obtained using GRASP2K [42], to an accuracy of 10^{-4} hartree or lower. To determine the optimal orbital basis set, we compute α with increasing basis size and the results are listed in Table. IV. From the table, we observe convergence of α up to 10^{-3} a.u. with a basis set of 171 orbitals. Based on the results, we choose the set with 135 orbitals as the optimal one and use it for more detailed studies.

In Table. V the converged values of α along with the previous theoretical results and experimental data are listed for comparison. From the table it is evident that our result of 38.72 is in very good agreement with the experimental value of 38.8(8). Among the previous theoretical results, the results from configuration interaction with a semi-empirical core-polarization potential (CICP) [49] is on the lower side. There are two other theoretical results based on coupled-cluster theory. The first [50] is using non-relativistic Hamiltonian with finite field approach, where as the second [51] uses Dirac-Coulomb Hamiltonian with the external electric field treated as a perturbation. In both the works, the contributions from triple excitations are included perturbatively. Compared to the experimental value, the results from the first work [50] is on the higher side, but the result from the second work [51] is close to the experimental value. The method used in ref. [51] is similar, in the way the external field is treated as a perturbation and computation of a second set of cluster amplitudes, to PRCC. However, our result is in better agreement with the experimental value. This may be on account of two important factors: inclusion of Breit-interaction in the atomic Hamiltonian and computation of $T_3^{(0)}$ without perturbative approximations. With the inclusion of perturbative $T_3^{(1)}$, result listed as PRCC(T) in Table. V, our result is in excellent agreement with the experimental data.

The term wise contribution to α in Eq. (25) are listed in Table. VI. From the table the LO contribution arises

from $\mathbf{T}_1^{(1)\dagger} \mathbf{D} + \text{H.c.}$ and is larger than the total value of α . This is, perhaps, not surprising as the LO term subsumes the Dirac-Hartree-Fock contribution and core-polarization effects. The next to leading order (NLO) is $\mathbf{T}_1^{(1)\dagger} \mathbf{D} T_1^{(0)} + \text{H.c.}$, and opposite in phase to the LO. A similar phase relation between the LO and NLO was observed in our previous work on noble gas [22] and alkaline-Earth-metal [25] atoms. Among the remaining terms, the contribution from $\mathbf{T}_1^{(1)\dagger} \mathbf{D} T_2^{(0)} + \text{H.c.}$ is similar in value and phase to the NLO term. The sub-shell wise contributions from the LO term, as mentioned earlier is the sum of $\mathbf{T}_1^{(1)\dagger} \mathbf{D}$ and its hermitian conjugate, are listed in Table. VII. From the table, the valence sub-shell $4s_{1/2}$ is the most dominant, and followed by $3d_{5/2}$. Both the sub-shell contributions have same phase, and together accounts for more than 99% of the LO term.

TABLE V. Static dipole polarizability α of Zn, Cd and Hg in atomic units (a_0^3).

Atom	Present	Method	Previous Works	Method
Zn	38.72	PRCC	38.12[49]	CICP
	38.76	PRCC(T)	38.5[52]	MCSCF
			38.4[53]	CASPT2
			37.86[54]	CCSD(T)
			38.01[55]	CCSD(T)
			39.2(8)[50]	CCSD(T)
			38.666(35)[51]	RCCSD _p T
			38.8(8)[50]	Expt.
			38.92 ^a	Expt.
			44.63[49]	CICP
Cd	49.11	PRCC	46.9[53]	CASPT2
	49.20	PRCC(T)	47.63[54]	CCSD(T)
			46.25[55]	CCSD(T)
			45.856(42)[51]	RCCSD _p T
			49.65(1.47)[56]	Expt.
			49.50 ^a	Expt.
			50.0(2.8) ^b	Expt.
			31.32[49]	CICP
			33.3[53]	CASPT2
			33.44[57]	QCISD(T)
Hg	33.50	PRCC	31.82[54]	CCSD(T)
	33.59	PRCC(T)	34.42[55]	CCSD(T)
			34.15[58]	CCSD(T)
			33.6[59]	CI + MBPT
			33.7(1.3) ^c	Expt.
			33.75 ^d	Expt.
			33.91(34)[60]	Expt.

^a Reference [61] based on experimental data in Ref. [50, 56].

^b Reference [56] based on the refractive index data in Ref. [62].

^c Reference [60] based on the dielectric data in Ref. [63].

^d Reference [64] based on the experimental data in Ref. [60].

B. Cd

The corrections to the orbitals energies $\Delta\epsilon_{\text{Br}}$ and $\Delta\epsilon_{\text{Ue}}$ arising from Breit-interaction and Uehling potential, respectively, are listed in Table. III. From the table it is evident that like in Zn $\Delta\epsilon_{\text{Br}}$ of the $4d_{5/2}$, the sub-shell next to the valence, is negative. Over all the general trend in the corrections is very similar to the case of Zn, except that the magnitude of the corrections are one order higher. There is, however, one noticeable change in the relative values of $\Delta\epsilon_{\text{Ue}}$ for the $p_{1/2}$ and $p_{3/2}$ orbitals. In the case of Zn, $\Delta\epsilon_{\text{Ue}(mp_{1/2})} \approx \Delta\epsilon_{\text{Ue}(mp_{3/2})}$ (with $m = 2, 3$), but in the Cd, $\Delta\epsilon_{\text{Ue}(mp_{1/2})}$ is about a factor of two smaller than $\Delta\epsilon_{\text{Ue}(mp_{3/2})}$. This indicates an enhanced effect of the Uehling potential or vacuum polarization potential to the inner $p_{1/2}$ orbitals with higher nuclear charge Z . It is an expected trend as the $p_{1/2}$ orbitals contract with higher Z due to larger relativistic corrections, and the inner orbitals contract more as the correction is larger.

TABLE VI. Contribution to α from different terms and their hermitian conjugates in the PRCC theory in atomic units (a_0^3).

Terms + h.c.	Zn	Cd	Hg
$\mathbf{T}_1^{(1)\dagger} \mathbf{D}$	45.590	61.456	41.927
$\mathbf{T}_1^{(1)\dagger} \mathbf{D} T_2^{(0)}$	-1.850	-3.128	-2.724
$\mathbf{T}_2^{(1)\dagger} \mathbf{D} T_2^{(0)}$	1.364	2.060	1.504
$\mathbf{T}_1^{(1)\dagger} \mathbf{D} T_1^{(0)}$	-1.901	-3.808	-1.583
$\mathbf{T}_2^{(1)\dagger} \mathbf{D} T_1^{(0)}$	0.081	0.243	0.091
Normalization	1.118	1.157	1.171
Total	38.716	49.112	33.499

Like in the case of Zn, orbital energies of Cd corresponding to the GTOs and numerical results from GRASP2K [42] are listed in the Table. III. It is evident that the basis parameters chosen for the Cd basis matches the orbital energies with the numerical results to within $10^{-4} - 10^{-3}$ hartrees. On comparison, on an average the agreement is in the case of Zn an order of magnitude better. This is on account of the larger number of occupied orbitals Cd, which increases the parameters of optimization. Coming to the results of α , from Table. IV, we find that α converges to $\approx 10^{-3}$ a. u. with a basis set of 165 orbitals. However, considering the number of cluster amplitudes, we take the basis set consisting of 143 orbitals for further computations. It must be mentioned that, with this basis set the convergence of α is $\approx 10^{-2}$ a. u..

From the results listed in Table. V, it is evident that there is a variation in the previous results from coupled-cluster theory. There are three previous theoretical works on the computation of α using coupled-cluster theory [51, 54, 55]. However, each of these use different types of basis sets, Ref. [54] and [55] are based on optimization

with polarization potential and pseudo-potential, respectively. In terms of the theory and type of basis functions, the methods we have used in the present work is very similar to Ref. [51]. There is, however, noticeable difference between the two results, and this may be due to difference in the methods at various stages of computations. For the present work, as described earlier, we have provided detailed information about the basis set parameters, and convergence of α with the basis size. It must be emphasized that our result for α is closest to the experimental value. The agreement with the experimental data improves with the inclusion of perturbative $\mathbf{T}_3^{(1)}$, the result listed as PRCC(T) in Table. V. The term wise contribution to α as listed in Table. VI has the same trend, albeit larger values, as in Zn. Coming to the sub-shell contributions to the LO term, from the values listed in Table. VII the pattern is similar to Zn: the dominant contribution arises from the valence sub-shell $5s_{1/2}$, and followed by $4d_{5/2}$, the sub-shell below the valence. However, compared to Zn, the dominant and next contribution in Cd are $\approx 25\%$ and $\approx 47\%$ larger, respectively.

TABLE VII. Four leading contributions to $\{\mathbf{T}_1^{(1)\dagger}\mathbf{D}\}$ to α in terms of the core spin-orbitals in atomic units (a_0^3).

Zn	Cd	Hg
22.244 ($4s_{1/2}$)	29.771 ($5s_{1/2}$)	17.768 ($6s_{1/2}$)
0.362 ($3d_{5/2}$)	0.678 ($4d_{5/2}$)	2.239 ($5d_{5/2}$)
0.193 ($3d_{3/2}$)	0.340 ($4d_{3/2}$)	0.965 ($5d_{3/2}$)
-0.001 ($3s_{1/2}$)	-0.004 ($4p_{3/2}$)	-0.009 ($5p_{3/2}$)

Concerning the experimental results, there is slight variation of the experimental uncertainty listed in the literature. In the original experimental work of Goebel and Hohm [56], the α of Cd is reported as $49.65 \pm 1.46 \pm 0.16$ a.u. Based on this result the experimental value is listed as 49.65 ± 1.46 , $49.65(1.49)$ and 49.65 ± 1.62 in Ref. [11], [9], and [65], respectively. However, the quadrature of the uncertainties reported in Ref. [56] gives the result $49.65(1.47)$, the value listed in Table. V of the present work. This is a minor issue and does not impact on the experimental results. We have mentioned this to explain the difference in the experimental result of Cd listed in Table. V from the previous works, namely Ref. [11], [9] and [65].

One issue which require some consideration is the consistent lower values of α reported in the previous theoretical works when compared to the experimental data. A comprehensive overview of the experimental results indicates the value of 49.50 reported by Qiao and collaborators [61] based on the experimental data of Goebel and Hohm [56], we believe, is robust and reliable. This observation is based on three important considerations. First, the Wolfsohn's three term expression [66] used in Ref. [61], to calculate α from the frequency dependent dipole polarizability $\alpha(\omega)$, is an improvement over the

three term Cauchy expansion used in Ref. [56]. Second, the value 50.0(2.8) reported in Ref. [56], based on the refractive index data from the work of Cuthbertson and Metcalfe [62], is consistent with the results in Ref. [56, 61]. Finally, in the recent work of Hohm and Thakker [65], using a fitting function with second ionization energy and Waber-Cromer radius [67] as parameters, they arrive at the value of α for Cd as 50.72. This is very closed to the experimental values and must be given weightage as the values of α reported in Ref. [65], except for Hf, Pd and Hg, are in good agreement with the reliable theoretical and experimental results. So, there is consistency in the experimental, and semi-empirical results reported in the literature. This indicates the genesis of the lower theoretical results in the previous works must lie within the theoretical means and methods employed.

Returning to the wide variation in the theoretical results, the possible reason for this could be, as evident from Table. V Cd has the largest value of α among the group IIb elements. In addition, Z of Cd lies in the domain where relativistic effects begin to have an importance. So, in Cd, the relativistic and electron-correlation effects are inter-related strongly, as a result the properties which depend on electron correlation effects are sensitive to the choice of the basis set. One indication of this is the difference between the Hartree-Fock and CCSD(T) results of the α from the relativistic computations. From Ref. [55], this is found to be 17.12 which is larger than the corresponding values of 12.18 and 10.36 for Zn and Hg, respectively. This demonstrates the importance of the relativistic and correlation effects.

C. Hg

The results of Hg deserve detailed discussions as the current work is precursor to a refined recalculation of the Hg atomic EDM [68]. Like in the previous cases, the orbital energies of Hg and corrections are listed in Table. VIII. From the table it is evident that the values of $\Delta\epsilon_{\text{Br}}$ from the current work are in excellent agreement with the results reported in Ref. [1]. One noticeable change in the trend of $\Delta\epsilon_{\text{Br}}$ is the negative values of $\Delta\epsilon_{\text{Ue}(4f_{5/2})}$ and $\Delta\epsilon_{\text{Ue}(4f_{7/2})}$. In comparison, $\Delta\epsilon_{\text{Br}}$ is negative for $3d_{5/2}$ and $4d_{5/2}$ in Zn and Cd, respectively. The results seem to indicate that the outermost sub-shell with $j \geq 5/2$ have negative $\Delta\epsilon_{\text{Br}}$, which could be on account of the larger weight factor $(2j+1)$ associated with higher j in the exchange two-electron integrals. The reason behind this remark is, only the exchange integrals contribute to the $\Delta\epsilon_{\text{Br}}$ in closed-shell atoms and ions.

The Uehling potential corrections to the orbitals energies exhibit one marked change compared to Zn and Cd. In Hg, the values of $\Delta\epsilon_{\text{Ue}(mp_{1/2})}$ with $m = 2, 3, 4$ are negative. A similar result was reported for the case of Ra^{2+} in our previous work on doubly ionized alkaline-earth-metal atoms [24]. There is, however, one minor but important difference. In the case of Ra^{2+} the $\Delta\epsilon_{\text{Ue}}$

TABLE VIII. Orbital energies of Hg obtained from GRASP2K [42] and Gaussian type orbitals in atomic units. The quantities ΔE_{Br} and ΔE_{Ueh} are the orbital energy corrections arising from the Breit interaction and Uehling potential, respectively. In the table, [x] represents multiplication by 10^x . All the values are in atomic units (hartree).

Orbital	GRASP2K	DC	ΔE_{Br}		ΔE_{Ueh}
			Present	Ref. [1]	
$1s_{1/2}$	-3074.226 002	-3074.235 257	10.963 407	10.96	-1.557 141
$2s_{1/2}$	-550.251 032	-550.254 927	1.229 461	1.230	-2.206 016[-1]
$2p_{1/2}$	-526.854 793	-526.857 122	2.067 249	2.067	-1.415 186[-2]
$2p_{3/2}$	-455.156 786	-455.159 068	1.304 845	1.305	7.499 950[-3]
$3s_{1/2}$	-133.113 168	-133.116 535	2.275 130[-1]	2.276[-1]	-5.013 463[-2]
$3p_{1/2}$	-122.639 005	-122.640 349	3.933 351[-1]	3.933[-1]	-3.454 750[-3]
$3p_{3/2}$	-106.545 242	-106.546 285	2.346 877[-1]	2.347[-1]	2.184 390[-3]
$3d_{3/2}$	-89.436 975	-89.440 259	1.708 149[-1]	1.708[-1]	2.426 999[-3]
$3d_{5/2}$	-86.020 282	-86.023 564	1.098 651[-1]	1.098[-1]	2.298 568[-3]
$4s_{1/2}$	-30.648 324	-30.649 589	4.665 828[-2]	4.667[-2]	-1.258 914[-2]
$4p_{1/2}$	-26.124 024	-26.123 690	8.337 968[-2]	8.339[-2]	-7.139 890[-4]
$4p_{3/2}$	-22.188 555	-22.188 057	4.359 830[-2]	4.360[-2]	7.141 810[-4]
$4d_{3/2}$	-14.796 757	-14.797 894	2.297 811[-2]	2.297[-2]	7.153 100[-4]
$4d_{5/2}$	-14.052 597	-14.053 659	9.563 165[-3]	9.554[-3]	6.841 500[-4]
$4f_{5/2}$	-4.472 939	-4.472 953	-5.808 097[-3]	-5.816[-3]	5.019 090[-4]
$4f_{7/2}$	-4.311 769	-4.311 745	-1.148 315[-2]	-1.150[-2]	4.923 107[-4]
$5s_{1/2}$	-5.103 103	-5.103 080	7.030 344[-3]	7.033[-3]	-2.389 679[-3]
$5p_{1/2}$	-3.537 946	-3.537 438	1.212 951[-2]	1.213[-2]	3.017 200[-6]
$5p_{3/2}$	-2.842 014	-2.841 487	4.829 281[-3]	4.828[-3]	2.641 881[-4]
$5d_{3/2}$	-0.650 063	-0.649 907	2.431 914[-4]	2.394[-4]	2.060 225[-4]
$5d_{5/2}$	-0.574 649	-0.574 475	-1.088 398[-3]	-1.093[-3]	1.954 800[-4]
$6s_{1/2}$	-0.328 036	-0.327 943	4.584 067[-4]	4.575[-4]	-2.026 796[-4]

is negative for all the $p_{1/2}$ orbitals. Whereas in Hg, $5p_{1/2}$ orbital, the outermost $p_{1/2}$ orbital, has positive $\Delta\epsilon_{\text{Ue}}$. We attribute this to the larger relativistic effects in Ra^{2+} due to the stronger nuclear potential. Coming to the basis set parameters, the values we have chosen generates orbitals with energies within $10^{-4} - 10^{-3}$ hartree of the numerical orbital energies.

The PRCC computations with excitations from all the core sub-shells of Hg generate cluster amplitudes in excess of 10^7 when the basis size is ~ 160 . The computation of α , then, requires thousands of hours of compute time, and detailed studies on the convergence properties is unfeasible (with our existing facilities). To mitigate this computational conundrum we restrict the cluster amplitudes to excitations from the $(4-6)s$, $(4-5)p$, $(4-5)d$, and $4f$ core sub-shells. From the results listed in Table IV, the α of Hg converges to 33.499 with a basis size of 134 orbitals.

Among the previous theoretical results, three are based on coupled-cluster theory, and we discuss these in some detail. Consider first the CCSD(T) results of Kello and Sadlej [54], it is obtained with a polarized basis set, and correlating the $5d^{10}6s^2$ electrons. So, it is effectively 12 electron coupled-cluster calculations with relativistic corrections through the mass-velocity operator. Their result is lower than ours, and below the experimental data as well. They also mention that α decreases to 31.24 when the computations are done with larger number of correlated electrons, namely, $5s^25p^65d^{10}6s^2$. So, the primary reason for the difference may be the form of the relativis-

tic effects. The second result is based on the CCSD(T) work of Seth and collaborators [55] using a basis set generated with an optimized quasirelativistic pseudopotential [69]. Their result is close to the experimental value, but on the higher side. The estimate of the contributions from the triple excitation is 0.84, which is smaller than the value 1.43 listed in the work of Kello and Sadlej [54]. This indicates that the contribution from the triple excitation depends on the nature of basis set and form of the effective interaction to account for relativistic corrections. This is perhaps not surprising as the electron correlation effects subsumed through the cluster operators depend on the nature of the basis functions. The third or the last previous work [58] on α of Hg with CCSD(T) is the closest, in terms of theoretical approach, to our present work. The computations are based on the Dirac-Coulomb Hamiltonian, and their result is within the experimental uncertainty. In summary, there is a variation in the trend of the previous CCSD(T) results. The first [54] and second [55] reports values which are below and above all the experimental data, respectively. The result of the third work [58] is consistent with the experimental results. It must also be mentioned that all of these three previous works are based on finite field method.

In the present work, as mentioned earlier, we use the Dirac-Coulomb-Breit atomic Hamiltonian. So, the Breit interaction is an additional relativistic effect considered in the present work compared to the previous coupled-cluster works. We must, however, add that there are other relativistic effects like frequency dependent trans-

verse photon interaction not included in the present work. Our result of 33.50 is close, but below the experimental uncertainty of the most recent work [60]. With the inclusion of perturbative $\mathbf{T}_3^{(1)}$ we get 33.59, this improves the agreement with experimental data. Among the previous works, the results based on QCISD [57] and CI-MBPT [59] are in very good agreement with our result. In the latter case an important point is, the basis set is generated with V^{N-1} potential. Whereas all the other previous works and ours are with basis generated using V^N potential. Considering that the results from the recent works [55, 58, 59], and the present work are with different methods, the relative variance of the results ($\approx 0.6\%$) is low. This demonstrates the methods do consolidate important relativistic and many-body effects correctly. From this we can infer that the basis set, and PRCC(T) theory used in the present work is well suited for precision computation of properties like atomic electric dipole moment.

The term wise contribution, as listed in Table. VI, Hg exhibits a noticeable change in the trend. The NLO contribution arises from $\mathbf{T}_1^{(1)\dagger}\mathbf{D}\mathbf{T}_2^{(0)} + \text{H.c.}$, where as it is $\mathbf{T}_1^{(1)\dagger}\mathbf{D}\mathbf{T}_1^{(0)} + \text{H.c.}$ in Zn and Cd. We attribute this to the electron-correlation effects associated with the electrons in $5d$ shell, which enhances the cluster amplitude of $\mathbf{T}_2^{(0)}$. This is also reflected in the pattern of the core sub-shell contribution to the LO term, where there is a marked change in the trend compared to Zn and Cd. The contribution from the valence shell, $6s_{1/2}$, is $\approx 40\%$ smaller than the valence sub-shell contribution in Cd. However, the contribution from the next core sub-shell $5d_{5/2}$ is more than double of $4d_{5/2}$ in Cd. This is on account of the relativistic contraction of the $6s_{1/2}$ radial wavefunction.

For Hg, two experimental results are available in the literature. First is based on the data of dielectric constant reported in Ref. [63], and the other is based on the recent experimental measurement of Goebel and Hohm [60]. The two results are in very good agreement. There is another result [64] derived from the experimental data of Ref. [60] using the three term expression of Wolfsohn [66]. The reanalysis is in view of the findings in Ref. [70] and [71], which report the need for eight or more terms, compared to three in Ref. [60], in the Cauchy expansion of frequency dependent polarizability to obtain converged moments.

D. Uncertainty estimates

We have identified different sources of uncertainties in the present work. These arise from various approximations at different stages of the RCC and PRCC computations. The first two sources of uncertainties are associated with the truncation of the basis set, and consideration of cluster operators up to $\mathbf{T}_3^{(0)}$ in the RCC theory. These are, however, negligible as we consider a basis set

which gives converged results of α . The third source of uncertainty is the incomplete consideration of $\mathbf{T}_3^{(1)}$ as we include it perturbatively. To estimate an upper bound on this uncertainty, consider the case of Hg, where the contribution from perturbative $\mathbf{T}_3^{(1)}$ is $\approx 0.3\%$, and is the largest among the three atoms studied. Since the perturbative treatment is considering the most dominant term, we can assume an uncertainty of $\approx 0.3\%$ as the upper bound arising from the remaining contributions from $\mathbf{T}_3^{(1)}$. The fourth source of uncertainty is the truncation in the expression of α in Eq. (25), in which we retain terms up to second order in cluster operators. In one of our previous works [72], we have shown the contribution from the third and higher order terms in cluster amplitudes is negligible. So, the uncertainty from this can also be neglected. The last two sources of uncertainties are associated with the frequency dependent Breit interaction, and violation of no-virtual-pair approximation. In our previous work [25], we had estimated the upper bound on the contribution from frequency dependent Breit interaction to be 0.13% for Ra. For the present work too, as Ra has higher Z than Hg, we consider this as the upper bound on the uncertainty arising from frequency dependent Breit interaction. As the systems under study are neutral atoms the contribution from the latter, violation of no-virtual-pair approximation, is negligible. Combining these, we estimate the uncertainty in the results of Zn and Cd to below 0.5% . For Hg, an additional source of uncertainty is the restriction of excitations from the core sub-shells $(4-6)s$, $(4-5)p$, $(4-5)d$ and $4f$ in the converged basis set. Based on the computations with smaller basis set, but with excitations from all the core sub-shells, the upper bound on the uncertainty of the Hg results is 1.0% .

VI. CONCLUSION

We have computed the α of Zn, Cd and Hg, the elements of the group IIB, using PRCC and our results are in very good agreement with the experimental data. Among the three elements, our result of Cd is of significance as ours is the only theoretical result consistent with the experimental data. Based on the analysis of available experimental data, we conclude that α of Cd reported by Qiao and collaborators [61] is reliable. We attribute the lower values reported in the previous theoretical works to the choice of basis set, and the interplay of relativistic corrections with electron correlation effects. This is in contrast to the case of Zn and Hg, where the electron correlation, and relativistic corrections are predominant effects, respectively.

In the PRCC sector, we have considered the triple excitation cluster operator through the dominant contribution from the perturbative $\mathbf{T}_3^{(1)}$, and included it in the computation of α . This brings the level of electron correlation effects, in terms of excited state, in PRCC the-

ory on par with the RCCSDT theory we have developed and used. The present work is based on use of Dirac-Coulomb-Breit atomic Hamiltonian. In addition, we also consider the corrections from the Uehling potential, the leading order term in the vacuum polarization effects. So, we incorporate relativistic effects, albeit incomplete, better than the previous theoretical works. The relativistic effects left out in the present work include self-energy corrections, frequency dependent transverse photon interaction and Wichmann-Kroll potential. We shall examine these in detail in future works, and may be essential to reduce the uncertainties to below 0.5% in the properties calculations of high Z elements like Hg.

An important highlight associated with an integral part of the Hamiltonian we use, Breit interaction, is the orbital energy correction associated with it. Our results are in excellent agreement with the previous results we could find in the literature, that is for Hg. This, we consider, as a reliable validation of our implementation of Breit interactions. In future works, we shall report the application of PRCC theory to one- and two-valence systems. For which we have reported the results with unperturbed RCCSD theory [72, 73].

ACKNOWLEDGMENTS

We thank Arko Roy and Kuldeep Suthar for useful discussions. The results presented in the paper are based on the computations using the 3TFLOP HPC Cluster at Physical Research Laboratory, Ahmedabad.

Appendix A

The angular factors of the terms in the linearized RCCSDT equation of $T_1^{(0)}$ given in Eq. (15). In the expressions, j_i s are the total angular momenta of the orbitals, and the quantities $[j]$ represent $2j + 1$.

$$\begin{aligned}
 A_1 &= \delta_{j_q, j_b} (-1)^{j_q - j_b} \\
 A_2 &= (-1)^{j_p - j_b + k_1} \frac{\delta_{j_b, j_q} \delta_{j_a, j_p}}{\sqrt{[j_b][j_p]}} \\
 A_3 &= \frac{1}{2} (-1)^{j_b + j_q + j_c + j_p} \frac{\delta_{j_a, j_p}}{[k_1] \sqrt{[j_p]}} \\
 A_4 &= \frac{1}{2} (-1)^{j_b + j_q + j_c - j_p} \frac{\delta_{j_a, j_p}}{\sqrt{[j_p]}} \begin{Bmatrix} k_1 & j_b & j_q \\ k_2 & j_c & j_p \end{Bmatrix} \\
 A_5 &= (-1)^{j_b + j_q + j_r + j_p} \frac{\delta_{j_a, j_p}}{[k_1] \sqrt{[j_p]}} \\
 A_6 &= (-1)^{j_r + j_p + j_q - j_b} \frac{\delta_{j_a, j_p}}{\sqrt{[j_p]}} \begin{Bmatrix} k_1 & j_r & j_b \\ k_2 & j_q & j_p \end{Bmatrix} \\
 A_7 &= \frac{1}{2[k_1] \sqrt{[l_2]}} (-1)^{j_b + j_q + j_c + j_r}
 \end{aligned}$$

$$A_8 = \frac{1}{2\sqrt{[l_2]}} (-1)^{-j_b + j_r + j_c + j_q} \begin{Bmatrix} k_1 & j_b & j_r \\ l_2 & j_c & j_q \end{Bmatrix}$$

Appendix B

The angular factors of the terms in the linearized RCCSDT equation of $T_2^{(0)}$ given in Eq. (16).

$$\begin{aligned}
 B_1 &= \frac{\delta_{j_b, j_r}}{\sqrt{[j_b]}} \\
 B_2 &= \frac{\delta_{j_c, j_q}}{\sqrt{[j_c]}} \\
 B_3 &= (-1)^{j_a + j_p + j_b + j + q} \frac{1}{\sqrt{[k]}} \begin{Bmatrix} k_1 & j_a & j_c \\ j_p & k_2 & k \end{Bmatrix} \begin{Bmatrix} k_1 & j_d & j_b \\ j_q & k & k_2 \end{Bmatrix} \\
 B_4 &= (-1)^{j_a + j_p + j_b + j_q} \frac{1}{\sqrt{[k]}} \begin{Bmatrix} k_1 & j_p & j_r \\ j_a & k_2 & k \end{Bmatrix} \begin{Bmatrix} k_1 & j_s & j_q \\ j_b & k & k_2 \end{Bmatrix} \\
 B_5 &= \sum_{k_1} (-1)^{j_c + k + j_r} \begin{Bmatrix} j_a & j_c & k_1 \\ j_r & j_p & k \end{Bmatrix} \\
 B_6 &= (-1)^{j_a + j_p + j_b + j_q + l_1 + k_1 + k_2} [l_1] \begin{Bmatrix} k_1 & j_b & j_c \\ j_q & k_2 & l_1 \end{Bmatrix} \\
 &\quad \times \begin{Bmatrix} k_1 & j_r & j_p \\ j_a & l_1 & k_2 \end{Bmatrix} \\
 B_7 &= \frac{1}{2[k]} ((-1)^{j_r + k - j_c} \\
 B_8 &= \frac{1}{2} (-1)^{j_c + k_1 + j_r} \begin{Bmatrix} j_c & j_q & k_1 \\ j_b & j_r & k \end{Bmatrix} \\
 B_9 &= (-1)^{j_r - j_c + j_b + j_q} \begin{Bmatrix} j_b & j_s & l_2 \\ l_1 & k & j_q \end{Bmatrix} \\
 B_{10} &= (-1)^{j_c + j_s + j_b + j_q + k + l_1} \begin{Bmatrix} k_1 & j_c & j_s \\ l_1 & j_q & j_r \end{Bmatrix} \begin{Bmatrix} j_b & j_s & l_2 \\ l_1 & k & j_q \end{Bmatrix} \\
 B_{11} &= \frac{1}{2[k]} (-1)^{j_r - j_c + j_b + j_q + l_2} \begin{Bmatrix} j_q & j_d & l_2 \\ l_1 & k & j_b \end{Bmatrix} \\
 B_{12} &= \frac{1}{2} (-1)^{j_c + j_r + j_b + j_q + l_2} \begin{Bmatrix} k_1 & j_r & j_d \\ l_1 & j_b & j_c \end{Bmatrix} \begin{Bmatrix} j_d & l_2 & j_q \\ k & j_b & l_1 \end{Bmatrix}
 \end{aligned}$$

Appendix C

The angular factors of the terms in the linearized RCCSDT equation of $T_3^{(0)}$ given in Eq. (17). It is to be that the expression of C_4 includes a $9j$ -symbol.

$$\begin{aligned}
 C_1 &= (-1)^{j_b + j_q + l_2} \begin{Bmatrix} l_3 & j_q & j_s \\ j_b & l_1 & l_2 \end{Bmatrix} \\
 C_2 &= (-1)^{j_b + j_q + l_3 + l_1} \begin{Bmatrix} l_3 & j_b & j_d \\ j_q & l_1 & l_2 \end{Bmatrix} \\
 C_3 &= (-1)^{j_s - j_d + l_1} \frac{1}{[l_1]}
 \end{aligned}$$

$$\begin{aligned}
C_4 &= (-1)^{j_b+2j_q+j_s+l_1} [l] \left\{ \begin{matrix} m_1 & l_3 & m_2 \\ j_b & l_2 & j_q \\ j_s & l_1 & j_d \end{matrix} \right\} \\
C_5 &= (-1)^{j_a+j_p+j_b+j_q+l_3} [l_1][l_2] \left\{ \begin{matrix} m_1 & j_s & j_a \\ j_p & l_1 & k \end{matrix} \right\} \\
&\quad \times \left\{ \begin{matrix} j_q & j_d & m_2 \\ k & l_2 & j_b \end{matrix} \right\} \left\{ \begin{matrix} m_2 & m_1 & l_3 \\ l_1 & l_2 & k \end{matrix} \right\} \\
C_6 &= (-1)^{j_d+j_s+l_1} \left\{ \begin{matrix} j_a & j_d & k \\ j_s & j_p & l_1 \end{matrix} \right\} \\
C_7 &= (-1)^{j_a+j_p+j_b+j_q+k+m_2+l_2+l_3} [l_1][l_2] \left\{ \begin{matrix} m_1 & j_s & j_a \\ j_p & l_1 & k \end{matrix} \right\} \\
&\quad \times \left\{ \begin{matrix} j_b & j_t & m_2 \\ k & l_2 & j_q \end{matrix} \right\} \left\{ \begin{matrix} m_2 & m_1 & l_3 \\ l_1 & l_2 & k \end{matrix} \right\} \\
C_8 &= (-1)^{j_a+j_p+j_b+j_q+k+m_1+l_1+l_3} [l_1][l_2] \left\{ \begin{matrix} m_1 & j_d & j_p \\ j_a & l_1 & k \end{matrix} \right\} \\
&\quad \times \left\{ \begin{matrix} j_q & j_e & m_2 \\ k & l_2 & j_b \end{matrix} \right\} \left\{ \begin{matrix} m_2 & m_1 & l_3 \\ l_1 & l_2 & k \end{matrix} \right\}
\end{aligned}$$

Appendix D

The angular factors of the terms in the linearized PRCC equation of $\mathbf{T}_1^{(1)}$ given in Eq. (21).

$$\begin{aligned}
\mathcal{A}_1 &= \frac{\delta(j_a, j_q)}{\sqrt{[j_a]}} \\
\mathcal{A}_2 &= \frac{\delta(j_b, j_p)}{\sqrt{[j_b]}} \\
\mathcal{A}_3 &= \frac{1}{\sqrt{3}} (-1)^{j_q-j_b+1} \\
\mathcal{A}_4 &= (-1)^{j_b+j_q+1} \left\{ \begin{matrix} j_b & j_q & 1 \\ j_a & j_p & k \end{matrix} \right\} \\
\mathcal{A}_5 &= \frac{1}{\sqrt{3}} (-1)^{j_q-j_b+k_1} \\
\mathcal{A}_6 &= (-1)^{j_b+j_q+1} \left\{ \begin{matrix} j_a & j_b & k \\ j_q & j_p & 1 \end{matrix} \right\} \\
\mathcal{A}_7 &= \frac{1}{\sqrt{[m_2]}} (-1)^{j_q-j_b+j_a+j_p+m_1} \left\{ \begin{matrix} j_r & j_a & m_1 \\ 1 & m_2 & j_p \end{matrix} \right\} \\
\mathcal{A}_8 &= (-1)^{j_a+j_p+j_b+j_q+m_1} \left\{ \begin{matrix} j_b & k & j_r \\ j_p & m_2 & j_q \end{matrix} \right\} \left\{ \begin{matrix} j_r & j_a & m_1 \\ 1 & m_2 & j_p \end{matrix} \right\} \\
\mathcal{A}_9 &= \frac{1}{\sqrt{[m_2]}} (-1)^{j_a-j_b+j_p+j_q+1+m_2} \left\{ \begin{matrix} j_p & m_1 & j_c \\ m_2 & j_a & 1 \end{matrix} \right\}
\end{aligned}$$

$$\mathcal{A}_{10} = (-1)^{j_q+j_c+j_a+j_p+1+m_2} \left\{ \begin{matrix} k & j_a & j_c \\ m_2 & j_q & j_b \end{matrix} \right\} \left\{ \begin{matrix} j_b & j_p & m_1 \\ 1 & m_2 & j_a \end{matrix} \right\},$$

Appendix E

The angular factors of the terms in the linearized PRCC equation of $\mathbf{T}_2^{(1)}$ given in Eq. (21).

$$\begin{aligned}
\mathcal{B}_1 &= [l_1] (-1)^{j_a+j_p+1+l_2} \left\{ \begin{matrix} 1 & j_p & j_r \\ j_a & l_2 & l_1 \end{matrix} \right\} \\
\mathcal{B}_2 &= [l_1] (-1)^{j_a+j_p+l_1} \left\{ \begin{matrix} 1 & j_a & j_c \\ j_p & l_2 & l_1 \end{matrix} \right\} \\
\mathcal{B}_3 &= [l_1] (-1)^{j_a+j_p+l_1} \left\{ \begin{matrix} l_2 & j_p & j_r \\ j_a & 1 & l_1 \end{matrix} \right\} \\
\mathcal{B}_4 &= [l_1] (-1)^{j_a+j_p+1+l_2} \left\{ \begin{matrix} l_2 & j_a & j_c \\ j_p & 1 & l_1 \end{matrix} \right\} \\
\mathcal{B}_5 &= \frac{1}{[l_1]} (-1)^{j_r-j_c+l_1} \\
\mathcal{B}_6 &= [l_2] (-1)^{j_c-j_q+1+m_2} \left\{ \begin{matrix} j_r & m_1 & j_b \\ j_c & m_2 & j_q \\ l_1 & 1 & l_2 \end{matrix} \right\} \\
\mathcal{B}_7 &= [l_1][l_2] (-1)^{j_a+j_p+j_b+j_q+1} \left\{ \begin{matrix} k & j_p & j_r \\ j_a & m_1 & l_1 \end{matrix} \right\} \\
&\quad \times \left\{ \begin{matrix} l_2 & l_1 & 1 \\ m_1 & m_2 & k \end{matrix} \right\} \left\{ \begin{matrix} k & j_c & j_b \\ j_q & l_2 & m_2 \end{matrix} \right\} \\
\mathcal{B}_8 &= (-1)^{j_c+j_r+l_1} \left\{ \begin{matrix} j_a & j_c & k \\ j_r & j_p & l_1 \end{matrix} \right\} \\
\mathcal{B}_9 &= [l_1][l_2] (-1)^{j_a+j_p+j_b+j_q+1+k+l_2+m_2} \left\{ \begin{matrix} k & j_p & j_r \\ j_a & l_1 & m_1 \end{matrix} \right\} \\
&\quad \times \left\{ \begin{matrix} m_1 & l_1 & k \\ l_2 & m_2 & 1 \end{matrix} \right\} \left\{ \begin{matrix} k & j_s & j_q \\ j_b & m_2 & l_2 \end{matrix} \right\} \\
\mathcal{B}_{10} &= [l_1][l_2] (-1)^{j_a+j_p+j_b+j_q+1+k+m_1+l_1} \left\{ \begin{matrix} k & j_a & j_c \\ j_p & m_1 & l_1 \end{matrix} \right\} \\
&\quad \times \left\{ \begin{matrix} l_2 & l_1 & 1 \\ m_1 & m_2 & k \end{matrix} \right\} \left\{ \begin{matrix} k & j_d & j_b \\ j_q & l_2 & m_2 \end{matrix} \right\}
\end{aligned}$$

-
- [1] E. Lindroth, A. M. Martensson-Pendrill, A. Ynnerman, and P. Oster, *J. Phys. B* **22**, 2447 (1989).
[2] K. Bonin and V. Kresin, *Electric-Dipole Polarizabilities of Atoms, Molecules and Clusters* (World Scientific Publ., Singapore, 1997).

- [3] M. Safronova, M. Kozlov, and C. Clark, *Ultrasonics, Ferroelectrics and Frequency Control*, *IEEE Transactions on* **59**, 439 (2012).
[4] S. A. Diddams, J. C. Bergquist, S. R. Jefferts, and C. W. Oates, *Science* **306**, 1318 (2004).

- [5] M. Takamoto, F.-L. Hong, R. Higashi, and H. Katori, *Nature* **435**, 321 (2005).
- [6] S. A. Diddams, T. Udem, J. C. Bergquist, E. A. Curtis, R. E. Drullinger, L. Hollberg, W. M. Itano, W. D. Lee, C. W. Oates, K. R. Vogel, and D. J. Wineland, *Science* **293**, 825 (2001).
- [7] G. Wilpers, T. Binnewies, C. Degenhardt, U. Sterr, J. Helmcke, and F. Riehle, *Phys. Rev. Lett.* **89**, 230801 (2002).
- [8] W. C. Griffith, M. D. Swallows, T. H. Loftus, M. V. Romalis, B. R. Heckel, and E. N. Fortson, *Phys. Rev. Lett.* **102**, 101601 (2009).
- [9] J. Mitroy, M. S. Safronova, and C. W. Clark, *J. Phys. B* **43**, 202001 (2010).
- [10] Available as pdf file from the CTCP website at Massey University: <http://ctcp.massey.ac.nz/dipole-polarizabilities>.
- [11] P. Schwerdtfeger, “Atomic static dipole polarizabilities,” in *Computational Aspects of Electric Polarizability Calculations: Atoms, Molecules and Clusters*, edited by G. Maroulis (IOS Press, Amsterdam, 2006) pp. 1–32.
- [12] F. Coester, *Nucl. Phys.* **7**, 421 (1958).
- [13] F. Coester and H. Kümmel, *Nucl. Phys.* **17**, 477 (1960).
- [14] J. Čížek, *Adv. Chem. Phys.* **14**, 3589 (1969).
- [15] R. Pal, M. S. Safronova, W. R. Johnson, A. Derevianko, and S. G. Porsev, *Phys. Rev. A* **75**, 042515 (2007).
- [16] B. K. Mani, K. V. P. Latha, and D. Angom, *Phys. Rev. A* **80**, 062505 (2009).
- [17] H. S. Nataraj, B. K. Sahoo, B. P. Das, and D. Mukherjee, *Phys. Rev. Lett.* **106**, 200403 (2011).
- [18] T. A. Isaev, A. N. Petrov, N. S. Mosyagin, A. V. Titov, E. Eliav, and U. Kaldor, *Phys. Rev. A* **69**, 030501 (2004).
- [19] G. Hagen, T. Papenbrock, A. Ekström, K. A. Wendt, G. Baardsen, S. Gandolfi, M. Hjorth-Jensen, and C. J. Horowitz, *Phys. Rev. C* **89**, 014319 (2014).
- [20] P. H. Y. Li, R. F. Bishop, and C. E. Campbell, *Phys. Rev. B* **89**, 220408 (2014).
- [21] S. Chattopadhyay, B. K. Mani, and D. Angom, *Phys. Rev. A* **86**, 022522 (2012).
- [22] S. Chattopadhyay, B. K. Mani, and D. Angom, *Phys. Rev. A* **86**, 062508 (2012).
- [23] S. Chattopadhyay, B. K. Mani, and D. Angom, *Phys. Rev. A* **87**, 042520 (2013).
- [24] S. Chattopadhyay, B. K. Mani, and D. Angom, *Phys. Rev. A* **87**, 062504 (2013).
- [25] S. Chattopadhyay, B. K. Mani, and D. Angom, *Phys. Rev. A* **89**, 022506 (2014).
- [26] B. K. Sahoo and B. P. Das, *Phys. Rev. A* **77**, 062516 (2008).
- [27] Y. Singh, B. K. Sahoo, and B. P. Das, *Phys. Rev. A* **88**, 062504 (2013).
- [28] P. J. Mohr, B. N. Taylor, and D. B. Newell, *Rev. Mod. Phys.* **84**, 1527 (2012).
- [29] R. E. Stanton and S. Havriliak, *J. Chem. Phys.* **81**, 1910 (1984).
- [30] A. K. Mohanty and E. Clementi, *J. Chem. Phys.* **93**, 1829 (1990).
- [31] I. Grant, in *Springer Handbook of Atomic, Molecular, and Optical Physics*, edited by G. Drake (Springer, New York, 2006) pp. 325–357.
- [32] I. P. Grant, *Relativistic Quantum Theory of Atoms and Molecules: Theory and Computation* (Springer, New York, 2010).
- [33] G. D. Purvis and R. J. Bartlett, *J. Chem. Phys.* **76**, 1910 (1982).
- [34] I. Lindgren and J. Morrison, *Atomic Many-Body Theory* (Springer, Berlin, 2nd Edition, 1986).
- [35] A. Derevianko, S. G. Porsev, and K. Beloy, *Phys. Rev. A* **78**, 010503(R) (2008).
- [36] W. Johnson, *Atomic Structure Theory: Lectures on Atomic Physics* (Springer, Berlin, 2007).
- [37] S. A. Blundell, W. R. Johnson, Z. W. Liu, and J. Sapirstein, *Phys. Rev. A* **39**, 3768 (1989).
- [38] A. K. Mohanty, F. A. Parpia, and E. Clementi, in *Modern Techniques in Computational Chemistry: MOTECC-91*, edited by E. Clementi (ESCOM, 1991).
- [39] Y. Ishikawa, H. M. Quiney, and G. L. Malli, *Phys. Rev. A* **43**, 3270 (1991).
- [40] H. M. Quiney, in *Handbook of Molecular Physics and Quantum Chemistry*, Vol. 2, edited by S. Wilson, P. P. Bernath, and R. McWeeny (John Wiley & Sons Ltd., Chichester, 2003) pp. 444–483.
- [41] R. K. Chaudhuri, P. K. Panda, and B. P. Das, *Phys. Rev. A* **59**, 1187 (1999).
- [42] P. Jönsson, G. Gaigalas, J. Bieroń, C. Froese Fischer, and I. P. Grant, *Comp. Phys. Comm.* **184**, 2197 (2013).
- [43] C. Froese Fischer, *Comp. Phys. Comm.* **43**, 355 (1987).
- [44] Y. Ishikawa and K. Koc, *Phys. Rev. A* **50**, 4733 (1994).
- [45] P. Pulay, *Chem. Phys. Lett.* **73**, 393 (1980).
- [46] I. P. Grant and N. C. Pyper, *J. Phys. B* **9**, 761 (1976).
- [47] I. P. Grant and B. J. McKenzie, *J. Phys. B* **13**, 2671 (1980).
- [48] J. B. Mann and W. R. Johnson, *Phys. Rev. A* **4**, 41 (1971).
- [49] A. Ye and G. Wang, *Phys. Rev. A* **78**, 014502 (2008).
- [50] D. Goebel, U. Hohm, and G. Maroulis, *Phys. Rev. A* **54**, 1973 (1996).
- [51] Y. Singh and B. K. Sahoo, arXiv:1405.4950.
- [52] M. E. Rosenkrantz, W. J. Stevens, M. Krauss, and D. D. Konowalow, *J. Chem. Phys.* **72**, 2525 (1980).
- [53] B. O. Roos, R. Lindh, P. Malmqvist, V. Veryazov, and P. Widmark, *J. Phys. Chem. A* **109**, 6575 (2005).
- [54] V. Kellö and A. Sadlej, *Theor. Chim. Acta* **91**, 353 (1995).
- [55] M. Seth, P. Schwerdtfeger, and M. Dolg, *J. Chem. Phys.* **106**, 3623 (1997).
- [56] D. Goebel and U. Hohm, *Phys. Rev. A* **52**, 3691 (1995).
- [57] P. Schwerdtfeger, J. Li, and P. Pyrkö, *Theor. Chim. Acta* **87**, 313 (1994).
- [58] V. Pershina, A. Borschevsky, E. Eliav, and U. Kaldor, *J. Chem. Phys.* **128**, 024707 (2008).
- [59] H. Hachisu, K. Miyagishi, S. G. Porsev, A. Derevianko, V. D. Ovsiannikov, V. G. Pal’chikov, M. Takamoto, and H. Katori, *Phys. Rev. Lett.* **100**, 053001 (2008).
- [60] D. Goebel and U. Hohm, *J. Phys. Chem.* **100**, 7710 (1996).
- [61] L. W. Qiao, P. Li, and K. T. Tang, *J. Chem. Phys.* **137**, 084309 (2012).
- [62] C. Cuthbertson and E. P. Metcalfe, *Phil. Trans. R. Soc. Lond. A* **207**, 135 (1908).
- [63] P. Wüsthoff, *Ann. der Physik* **27**, 312 (1936).
- [64] K. Tang and J. Toennies, *Mol. Phys.* **106**, 1645 (2008).
- [65] U. Hohm and A. J. Thakker, *Phys. Chem. A* **116**, 697 (2012).
- [66] G. Wolfsohn, *Z. Physik* **83**, 234 (1933).
- [67] J. T. Waber and D. T. Cromer, *J. Chem. Phys.* **42**, 4116 (1965).

- [68] K. V. P. Latha, D. Angom, B. P. Das, and D. Mukherjee, [Phys. Rev. Lett. **103**, 083001 \(2009\)](#).
- [69] P. Schwerdtfeger, L. v. Szentpaly, K. Vogel, H. Silberbach, H. Stoll, and H. Preuss, [J. Chem. Phys. **84**, 1606 \(1986\)](#).
- [70] P. Salek, T. Helgaker, and T. Saue, [Chemical Physics **311**, 187 \(2005\)](#).
- [71] N. Gaston, P. Schwerdtfeger, T. Saue, and J. Greif, [J. Chem. Phys. **124**, 044304 \(2006\)](#).
- [72] B. K. Mani and D. Angom, [Phys. Rev. A **81**, 042514 \(2010\)](#).
- [73] B. K. Mani and D. Angom, [Phys. Rev. A **83**, 012501 \(2011\)](#).